# Nonsmooth continuation of parameter dependent static contact problems with Coulomb friction

Jaroslav Haslinger[a], Vladimír Janovský[a], Radek Kučera[*,b], Kristina Motyčková[b]

[a] *KNM MFF UK, Sokolovská 83, 18675 Praha 8, CZ*
[b] *VŠB-TU Ostrava, 17. listopadu 15/2172, 708 33 Ostrava-Poruba, CZ*

**Abstract**

The paper presents a new variant of a nonsmooth continuation algorithm by means of which one can follow branches of solutions to 2D contact problems with Coulomb friction which are parameterized by the coefficient of friction. The algorithm is based on the predictor-corrector technique and uses the active set strategy implementation of the semismooth Newton method.

*Keywords:* contact problem, Coulomb friction, semismooth Newton method, nonsmooth continuation, multiple solutions
*2000 MSC:* 74B20, 74M15, 74M10, 74G35, 74G15

## 1. Introduction

Static contact problems with Coulomb friction represent a very hard theoretical problem. Their mathematical model leads to the so-called implicit variational inequality. The existence of at least one solution for any load vector has been shown provided that the coefficient of friction $\mathcal{F}$ is small enough and some additional smoothness assumptions on data are satisfied. The detailed mathematical analysis involving also quasistatic and dynamic contact problems can be found in [6]. On the other hand almost nothing is known on the structure of the solution set. Partial results concerning

[*]Corresponding author
*Email addresses:* hasling@karlin.mff.cuni.cz (Jaroslav Haslinger), janovsky@karlin.mff.cuni.cz (Vladimír Janovský), radek.kucera@vsb.cz (Radek Kučera[*,]), kristina.motyckova@vsb.cz (Kristina Motyčková)

uniqueness/non-uniqueness are available if the solution exhibits specific properties (see [13, 21]). On the other hand, for discrete contact problems obtained by a suitable finite element approximation certain information on the structure of solutions exists. For example it is known that such problems have a solution for any $\mathcal{F}$ and this solution is unique provided that the coefficient of friction is below a critical value $\mathcal{F}_{\text{crit}}$. Unfortunately this critical value is mesh dependent, more precisely if the discretization parameter $h$ tends to zero then $\mathcal{F}_{\text{crit}}$ tends to zero as well. The explicit dependence of $\mathcal{F}_{\text{crit}}$ on $h$ has been studied for instance in [8, 12]. To analyze qualitative properties of the solution set, we use a continuation approach. We suppose that the coefficient of friction $\mathcal{F}$ is a function of a real parameter $\beta$, $\mathcal{F} : \beta \mapsto \mathcal{F}(\beta)$ which serves as the continuation parameter in the discrete problem. Let $\Psi : \beta \mapsto x(\beta)$ be the respective (generally set valued) solution map, where $x(\beta)$ is a solution to the contact problem for the coefficient of friction $\mathcal{F}(\beta)$ and $x(\beta_0)$ be a reference solution at $\beta_0$. It is known that except specific points, the solution map $\Psi$ defines a curve in a neighborhood of $\beta_0$, i.e. the problem has a locally unique solution there (see [14] for $\mathcal{F}(\beta) = const.$ along the contact part and [10] for $\mathcal{F}(\beta)$ depending also on the spatial variable). With this result at hand, tracking the solution branch would be principally possible. Unfortunately standard continuation techniques may fail since the branches are only piecewise smooth, in general, due to a nonsmooth character of the problem. In addition to nonsmoothness, there are yet another two specific features of the solution map: *(i)* resulting branches are not generally piecewise linear unlike the continuation by the load vector (for the continuation of piecewise linear maps we refer to [17, 2]), *(ii)* the solution path may be a disconnected set with several disjoint branches so that a technique how to "jump" from one branch to another has to be developed. The method presented in this paper is not a general method for nonsmooth optimization. It was designed just for the continuation in 2D contact problems for elastic bodies with Coulomb friction.

An algorithm for a numerical continuation of a piecevise smooth solution curve has been proposed in [10], Algorithm 5.1 (Piecewise smooth variant of the Moore-Penrose continuation, see e.g. [2] for this notion). It was designed to solve parameter dependent contact problems with Coulomb friction and tested on problems with just one or two contact nodes, see also [16]. In order to apply this algorithm to large scale problems one has to provide a reliable computation of the *positively oriented tangent*, see e.g. [10], in a generic point (i.e a point, where the problem is differentiable).

In [9] we used an algorithm based on *tangent continuation*, see [4], Algorithm 4.25. Note that the tangent continuation fails at a (differentiable) turning point (for this notion, see e.g. [5]). We assume that such smooth turning points are not present in our case. This assumption was satisfied in all examples we computed. The proposed algorithm was able to continue piecewise affine solution branches parametrized by the load vector due to its linear dependence on a continuation parameter. The new version of the continuation algorithm presented in this paper is able to follow general piecewise smooth branches, in particular solutions parametrized by the friction coefficient. The advantage of this variant is that branches (namely, their smooth pieces, see Section 5) are parametrized naturally by a chosen continuation parameter and not by quantities like an arclength, e.g.. The notion of an orientation is changed in our approach. The orientation (1 or $-1$) is assigned to each smooth piece in the process of continuation. A change of the orientation is linked to *turning transition points* where solutions change *qualitatively*, see Subsection 5.2. We also discuss the case when the problem depends on more than just one parameter, see Subsection 5.3.

An alternative continuation algorithm was recently proposed in [19]. It is based on the above mentioned Moore-Penrose continuation. Finding a positively oriented tangent at a nonsmooth point is a crucial step. This is done by the procedure called the Tangent Switch that is actually a heuristic rule. It is fair to say that also our new continuation procedure is based on generic assumptions, Subsection 5.2, ALGORITHM NSM (New Smooth Piece). The algorithm in [19] follows a path with a given orientation (in the classical sense), but it is not able to localize (in our notation) turning transition points.

The paper is organized as follows. In Section 2 we present the weak formulation of contact problems with Coulomb friction based on a fixed point approach. In order to release the unilateral constraints and to regularize the frictional term we introduce Lagrange multipliers. This leads to a new formulation of the problem in terms of displacements, normal and tangential contact stress which is next used in discretizations by finite elements. Two equivalent formulations of the discrete contact problem are presented: *(j)* as a generalized equation (GE), *(jj)* as a nonsmooth equation (NE). In Section 3 results on the existence of locally Lipschitz continuous branches of solutions parametrized by the coefficient of friction and the load vector are mentioned. Section 4 is devoted to the semismooth Newton method which uses the active set strategy for solving the problem expressed as (NE). The main part

of the paper is Section 5, where a new variant of the nonsmooth continuation algorithm is proposed. It consists of three parts: *(k)* predictor-corrector algorithm for the continuation along a smooth piece, *(kk)* the algorithm enabling us to detect a new smooth piece, *(kkk)* the algorithm used for finding another branches when the solution path is disconnected. Finally, Section 6 presents results of a model example computed by the proposed algorithm.

Throughout the paper we use the following notation. By $H^k(G)$, $k \geq 0$ integer we denote the classical Sobolev space of functions which are together with their generalized derivatives up to order $k$ square integrable in $G$ ($L^2(G) := H^0(G)$). Vectors, vector functions and spaces of vector functions will be denoted by bold characters: $\boldsymbol{x}$, $\boldsymbol{f}$, $\boldsymbol{V}$, etc.. $\mathbb{R}^s$, $s$ integer stands for the euclidean space of dimension $s$ ($\mathbb{R} := \mathbb{R}^1$) with the scalar product $(\cdot,\cdot)_s$ and the norm $\|\cdot\|_s = \sqrt{(\cdot,\cdot)_s}$. The max-norm of $\boldsymbol{x} \in \mathbb{R}^s$ will be denoted by $\|\cdot\|_{s,\infty}$. If $\boldsymbol{x} = (x_1,\ldots,x_s)^\top$, $\boldsymbol{y} = (y_1,\ldots,y_s)^\top$ are two vectors then $\boldsymbol{x} \geq \boldsymbol{y}$, $\boldsymbol{x} > \boldsymbol{y}$ means that $x_i \geq y_i$, and $x_i > y_i$, respectively $\forall i = 1,\ldots,s$ and $|\boldsymbol{x}| := (|x_1|,\ldots,|x_s|)$. Further $\mathbb{R}^s_+ = \{\boldsymbol{x} \in \mathbb{R}^s |\ \boldsymbol{x} \geq \boldsymbol{0}\}$ and $\mathbb{R}^s_{++} = \{\boldsymbol{x} \in \mathbb{R}^s |\ \boldsymbol{x} > \boldsymbol{0}\}$. If $\mathbb{A} = (a_{ij})$, $\mathbb{B} = (b_{ij})$ are two matrices of the same order then $\mathbb{A} : \mathbb{B} = \sum_{i,j} a_{ij} b_{ij}$.

## 2. Continuous and discrete settings of contact problems with Coulomb friction

This section starts with the presentation of the mechanical and mathematical model of contact problems with Coulomb friction. A mechanical system consists of two deformable bodies in mutual contact which are made of elastic materials. The bodies are represented by bounded domains $\Omega^1, \Omega^2 \subset \mathbb{R}^2$, the Lipschitz boundaries of which are split into three disjoint, non-empty parts: $\partial\Omega^j = \overline{\Gamma}^j_u \cup \overline{\Gamma}^j_f \cup \overline{\Gamma}^j_c$, $j = 1,2$. Denote $\Omega = \Omega^1 \cup \Omega^2$, $\Gamma_u = \Gamma^1_u \cup \Gamma^2_u$, $\Gamma_c = \Gamma^1_c \cup \Gamma^2_c$, and $\Gamma_f = \Gamma^1_f \cup \Gamma^2_f$. If a quantity $q$ is defined in $\Omega$, then its restriction to $\Omega^j$, or $\partial\Omega^j$ will be denoted by $q^j$, $j = 1,2$ in what follows. On different parts of $\partial\Omega$ different boundary conditions will be given. On $\Gamma_u$ the zero displacements will be prescribed while surface tractions of density $\boldsymbol{f}$ act on $\Gamma_f$. $\Gamma^j_c$ is a part of $\Omega^j$ along which both bodies may come into a contact. Next we shall suppose that $\Gamma^1_c = \Gamma^2_c$, i.e. there is no gap between $\Omega^1$ and $\Omega^2$ in the undeformed state. On the contact zone $\Gamma_c$ the influence of friction obeying Coulomb law will be taken into account. Finally, $\Omega$ is subject to body forces of density $\boldsymbol{F}$. Our aim is to find an equilibrium state of $\Omega$.

Before we give the mathematical model, we introduce several notation. By $\boldsymbol{\nu}$, $\boldsymbol{t}$ we denote the unite outward normal and tangential vector to $\partial\Omega$, respectively. According by to our convention, the symbols $\boldsymbol{\nu}^j$, $\boldsymbol{t}^j$ stand for the ones to $\partial\Omega^j$, $j = 1, 2$. In particular, $\boldsymbol{\nu}^1 = -\boldsymbol{\nu}^2$ on $\Gamma_c$. Further $\mathcal{F} := \mathcal{F}(\boldsymbol{x})$ is the coefficient of Coulomb friction which may depend on the spatial variable $\boldsymbol{x} \in \Gamma_c$.

By a *classical solution* of contact problems with Coulomb friction we mean any displacement vector $\boldsymbol{u} : \Omega \mapsto \mathbb{R}^2$ solving the following system of equations and boundary conditions:

- *(equilibrium equation)*

$$div\, \sigma(\boldsymbol{u}) + \boldsymbol{F} = \boldsymbol{0} \quad \text{in } \Omega, \tag{1}$$

- *(linear Hook's law)*

$$\sigma(\boldsymbol{u}) = C\varepsilon(\boldsymbol{u}), \quad \varepsilon(\boldsymbol{u}) = 1/2(\nabla \boldsymbol{u} + (\nabla \boldsymbol{u})^\top) \quad \text{in } \Omega, \tag{2}$$

- *(kinematical boundary condition)*

$$\boldsymbol{u} = \boldsymbol{0} \quad \text{on } \Gamma_u, \tag{3}$$

- *(static boundary condition)*

$$\boldsymbol{T}(\boldsymbol{u}) := \sigma(\boldsymbol{u})\boldsymbol{\nu} = \boldsymbol{f} \quad \text{on } \Gamma_f, \tag{4}$$

- *(transmission of contact stresses)*

$$\left.\begin{array}{l} \boldsymbol{T}_\nu(\boldsymbol{u}) := \sigma(\boldsymbol{u}^1)\boldsymbol{\nu}^1 \cdot \boldsymbol{\nu}^1 = \sigma(\boldsymbol{u}^2)\boldsymbol{\nu}^2 \cdot \boldsymbol{\nu}^2 \\ \boldsymbol{T}_t(\boldsymbol{u}) := \sigma(\boldsymbol{u}^1)\boldsymbol{\nu}^1 \cdot \boldsymbol{t}^1 = \sigma(\boldsymbol{u}^2)\boldsymbol{\nu}^2 \cdot \boldsymbol{t}^2 \end{array}\right\} \quad \text{on } \Gamma_c, \tag{5}$$

- *(contact conditions)*

$$u_\nu := (\boldsymbol{u}^1 - \boldsymbol{u}^2) \cdot \boldsymbol{\nu}^1 \leq 0,\ T_\nu(\boldsymbol{u}) \leq 0,\ u_\nu T_\nu(\boldsymbol{u}) = 0 \quad \text{on } \Gamma_c, \tag{6}$$

- *(Coulomb law of friction)*

$$\left.\begin{array}{l} |T_t(\boldsymbol{u})| \leq -\mathcal{F}T_\nu(\boldsymbol{u}) \\ u_t := (\boldsymbol{u}^1 - \boldsymbol{u}^2) \cdot \boldsymbol{t}^1 \neq 0 \Rightarrow T_t(\boldsymbol{u}) = \mathcal{F}T_\nu(\boldsymbol{u})\, sign\, u_t \end{array}\right\} \quad \text{on } \Gamma_c. \tag{7}$$

The symbol $C$ in (2) stands for the fourth order symmetric and elliptic elasticity tensor. Finally, $\sigma(\boldsymbol{u})$, $\varepsilon(\boldsymbol{u})$ is the stress and the strain tensor, respectively,

corresponding to $\boldsymbol{u}$ and $T_\nu(\boldsymbol{u})$, $T_t(\boldsymbol{u})$ in (5) is the normal and tangential component of the stress vector $\boldsymbol{T}(\boldsymbol{u})$ on $\Gamma_c$, respectively.

For theoretical and computational purposes we shall use a weak formulation of (1)-(7). To this end we introduce several notation. If $S(\Omega)$ is a space of functions defined in $\Omega$, then writing $v \in S(\Omega)$ we mean that $v^j \in S(\Omega^j)$, $j = 1, 2$ (and analogously for spaces of functions on $\partial\Omega$).

Let

$$\begin{aligned} V &= \{v \in H^1(\Omega) |\ v = 0 \text{ on } \Gamma_u\}, \\ \boldsymbol{V} &= V \times V, \\ \boldsymbol{K} &= \{\boldsymbol{v} \in \boldsymbol{V} |\ v_\nu \le 0 \text{ on } \Gamma_c\}. \end{aligned}$$

Denote by $\gamma_\nu, \gamma_t : \boldsymbol{V} \mapsto L^2(\Gamma_c)$ the trace mappings $\gamma_\nu : \boldsymbol{v} \mapsto v_\nu$, and $\gamma_t : \boldsymbol{v} \mapsto v_t$, respectively, on $\Gamma_c$, $\boldsymbol{v} \in \boldsymbol{V}$. Next we shall suppose that the boundaries $\partial\Omega^j$, $j = 1, 2$ are smooth so that $\gamma_\nu(\boldsymbol{V}) = \gamma_t(\boldsymbol{V}) \equiv X$. The dual space to $X$ will be denoted by $X'$, the cone of nonnegative functionals by $X'_+$ and the duality pairing on $X' \times X$ by $\langle \cdot, \cdot \rangle$. Finally,

$$\begin{aligned} a(\boldsymbol{u}, \boldsymbol{v}) &= \int_\Omega C\varepsilon(\boldsymbol{u}) : \varepsilon(\boldsymbol{v})\, d\boldsymbol{x}, \\ L(\boldsymbol{v}) &= \int_\Omega \boldsymbol{F} \cdot \boldsymbol{v}\, d\boldsymbol{x} + \int_{\Gamma_f} \boldsymbol{f} \cdot \boldsymbol{v}\, ds, \quad \boldsymbol{F} \in \boldsymbol{L}^2(\Omega),\ \boldsymbol{f} \in \boldsymbol{L}^2(\Gamma_f), \\ j(g, \boldsymbol{v}) &= \langle \mathcal{F} g, |v_t| \rangle \quad \forall \boldsymbol{u}, \boldsymbol{v} \in \boldsymbol{V},\ g \in X'_+. \end{aligned}$$

The coefficient of friction is represented by a positive function $\mathcal{F} \in C(\overline{\Gamma}_c)$ which is bounded from above: there exists $\mathcal{F}_{\max} > 0$ such that

$$0 < \mathcal{F}(\boldsymbol{x}) \le \mathcal{F}_{\max} \quad \forall \boldsymbol{x} \in \Gamma_c. \tag{8}$$

To get a weak formulation of (1)-(7) we use a fixed-point approach. To this end we consider the following auxiliary problem: given $g \in X'_+$

$$\left.\begin{aligned} &\text{Find } \boldsymbol{u} := \boldsymbol{u}(g) \in \boldsymbol{K} \text{ such that} \\ &a(\boldsymbol{u}, \boldsymbol{v} - \boldsymbol{u}) + j(g, \boldsymbol{v}) - j(g, \boldsymbol{u}) \ge L(\boldsymbol{v} - \boldsymbol{u}) \quad \forall \boldsymbol{v} \in \boldsymbol{K}. \end{aligned}\right\} \tag{$\mathcal{P}(g)$}$$

$(\mathcal{P}(g))$ is the weak formulation of contact problems with Tresca friction whose mathematical model is given by (1)-(7) with the following minor change in (7): the unknown normal stress $-T_\nu(\boldsymbol{u})$ is replaced by $g \in X'_+$. Problem $(\mathcal{P}(g))$ has a unique solution for any $g \in X'_+$ ([7, 11]).

Define a mapping $\Phi : X'_+ \mapsto X'_+$ by

$$\Phi(g) = -T_\nu(\boldsymbol{u}(g)) \in X'_+. \tag{9}$$

By a *weak solution* to contact problems with Coulomb friction we call any displacement vector $\boldsymbol{u}(g^*) \in \boldsymbol{K}$ which solves $(\mathcal{P}(g^*))$ with $g^* \in X'_+$ being a fixed point of $\Phi$ in $X'_+$: $\Phi(g^*) = g^* = -T_\nu(\boldsymbol{u}(g^*))$ on $\Gamma_c$.

**Remark 1.** It has been shown in [6] that if $\mathcal{F}_{\max}$ in (8) is sufficiently small and data of the problem are smooth enough then there exists at least one weak solution for any right hand side $L$.

To release the unilateral constraint $v_\nu \leq 0$ on $\Gamma_c$ and to regularize the functional $j$ in $(\mathcal{P}(g))$ we use a duality approach. Let

$$\begin{aligned} \Lambda_\nu &= X'_+, \\ \Lambda_t(g) &= \{\mu \in X' |\ \langle \mu, v_t\rangle + \langle \mathcal{F}g, |v_t|\rangle \geq 0\ \forall \boldsymbol{v} \in \boldsymbol{K}\}, \quad g \in \Lambda_\nu \end{aligned}$$

and define the problem:

$$\left.\begin{array}{l} \text{Find } (\boldsymbol{u}, \lambda_\nu, \lambda_t) := (\boldsymbol{u}(g), \lambda_\nu(g), \lambda_t(g)) \in \boldsymbol{V} \times \Lambda_\nu \times \Lambda_t(g) \text{ s.t.} \\ a(\boldsymbol{u}, \boldsymbol{v}) = L(\boldsymbol{v}) - \langle \lambda_\nu, v_\nu\rangle - \langle \lambda_t, v_t\rangle \quad \forall \boldsymbol{v} \in \boldsymbol{V}, \\ \langle \mu_\nu - \lambda_\nu, \mu_\nu\rangle + \langle \mu_t - \lambda_t, \mu_t\rangle \leq 0 \quad \forall (\mu_\nu, \mu_t) \in \Lambda_\nu \times \Lambda_t(g). \end{array}\right\} \quad (\mathcal{M}(g))$$

It is well known that also $(\mathcal{M}(g))$ has a unique solution for any $g \in X'_+$ and $(\boldsymbol{u}, \lambda_\nu, \lambda_t)$ solves $(\mathcal{M}(g))$ if and only if $\boldsymbol{u}$ solves $(\mathcal{P}(g))$ and $\lambda_\nu := -T_\nu(\boldsymbol{u})$, $\lambda_t := -T_t(\boldsymbol{u})$ on $\Gamma_c$ [11].

From the fixed-point formulation and using that $\lambda_\nu = -T_\nu(\boldsymbol{u})$ we obtain from $(\mathcal{M}(g))$ the following *primal-dual* formulation of contact problems with Coulomb friction:

$$\left.\begin{array}{l} \text{Find } (\boldsymbol{u}, \lambda_\nu, \lambda_t) \in \boldsymbol{V} \times \Lambda_\nu \times \Lambda_t(\lambda_\nu) \text{ such that} \\ a(\boldsymbol{u}, \boldsymbol{v}) = L(\boldsymbol{v}) - \langle \lambda_\nu, v_\nu\rangle - \langle \lambda_t, v_t\rangle \quad \forall \boldsymbol{v} \in \boldsymbol{V}, \\ \langle \mu_\nu - \lambda_\nu, \mu_\nu\rangle + \langle \mu_t - \lambda_t, \mu_t\rangle \leq 0 \quad \forall (\mu_\nu, \mu_t) \in \Lambda_\nu \times \Lambda_t(\lambda_\nu). \end{array}\right\} \quad (\mathcal{P})$$

Discretization of the problem will be based on the primal-dual formulation $(\mathcal{P})$. Next we describe the construction of $\boldsymbol{V}_h$, $\Lambda_{h\nu}$, $\Lambda_{ht}(g_h)$, $g_h \in \Lambda_{h\nu}$ being finite element discretizations of $\boldsymbol{V}$, $\Lambda_\nu$, and $\Lambda_t(g)$, respectively. To this end we shall suppose that $\Omega^j$ are *polygonal domains* with triangulations $\mathcal{T}_h^j$, $j = 1, 2$. Besides the standard assumptions on the mutual positions of

triangles $\Delta \in \mathcal{T}_h = \mathcal{T}_h^1 \cup \mathcal{T}_h^2$ we shall suppose that $\mathcal{T}_{h|\Gamma_c}^1 = \mathcal{T}_{h|\Gamma_c}^2$, i.e. the nodes of $\mathcal{T}_h^1$ and $\mathcal{T}_h^2$ on $\Gamma_c$ coincide. With any $\mathcal{T}_h$ we associate the space

$$\boldsymbol{V}_h = \{\boldsymbol{v}_h \in \boldsymbol{C}(\overline{\Omega})|\ \boldsymbol{v}_{h|\Delta} \in \boldsymbol{P}_1(\Delta)\ \ \forall \Delta \in \mathcal{T}_h,\ \boldsymbol{v}_h = \boldsymbol{0}\}, \quad \dim \boldsymbol{V}_h = n$$

and its convex subset

$$\boldsymbol{K}_h = \{\boldsymbol{v}_h \in \boldsymbol{V}_h|\ v_{h\nu}(\boldsymbol{a}_i) \le 0,\ \forall i = 1, \ldots, m\},$$

where $\boldsymbol{P}_1(\Delta)$ denotes the space of linear functions on $\Delta$ and $\{\boldsymbol{a}_i\}_{i=1}^m$ is the set of all contact nodes, i.e. the nodes of $\mathcal{T}_h$ lying on $\overline{\Gamma}_c \setminus \overline{\Gamma}_u$. The sets $\Lambda_{h\nu}$, $\Lambda_{ht}(g_h)$ will be generated by a finite collection $\{\delta_i\}_{i=1}^m$ of the Dirac distributions concentrated in the contact nodes, i.e. $\langle \delta_i, \varphi \rangle = \varphi(\boldsymbol{a}_i)$, $\varphi \in C(\overline{\Gamma}_c)$, $\forall i = 1, \ldots, m$:

$$\begin{aligned}
\Lambda_{h\nu} &= \{\mu_{h\nu}|\ \mu_{h\nu} = \sum_{i=1}^m \mu_{\nu i}\delta_i,\ \mu_{\nu i} \ge 0\ \forall i = 1, \ldots, m\},\\
\Lambda_{ht}(g_h) &= \{\mu_{ht}|\ \mu_{ht} = \sum_{i=1}^m \mu_{ti}\delta_i,\ |\mu_{ti}| \le (\mathcal{F}g)(\boldsymbol{a}_i)\ \forall i = 1, \ldots, m\}
\end{aligned}$$

assuming that $g \in C(\overline{\Gamma}_c)$. Any element $\mu_{h\nu} \in \Lambda_{h\nu}$, $\mu_{ht} \in \Lambda_{ht}(g_h)$ will be identified with the vectors $\boldsymbol{\mu}_\nu \in \boldsymbol{\Lambda}_\nu$, and $\boldsymbol{\mu}_t \in \boldsymbol{\Lambda}_t(\boldsymbol{g})$, respectively, formed by the coefficients of linear combination $\mu_{\nu i}$, $\mu_{ti}$, $i = 1, \ldots, m$.

It is readily seen that

$$\boldsymbol{\Lambda}_\nu = \mathbb{R}_+^m \quad \text{and} \quad \boldsymbol{\Lambda}_t(\boldsymbol{g}) = \{\boldsymbol{\mu}_t \in \mathbb{R}^m|\ |\boldsymbol{\mu}_t| \le \boldsymbol{\mathcal{F}} \odot \boldsymbol{g}\},$$

where $\boldsymbol{\mathcal{F}} = (\mathcal{F}_1, \ldots, \mathcal{F}_m)^\top$, $\boldsymbol{g} = (g_1, \ldots, g_m)^\top$, $\mathcal{F}_i := \mathcal{F}(\boldsymbol{a}_i)$, $g_i := g(\boldsymbol{a}_i)$, $i = 1, \ldots, m$, and $\boldsymbol{\mathcal{F}} \odot \boldsymbol{g} := (\mathcal{F}_1 g_1, \ldots, \mathcal{F}_m g_m)^\top \in \mathbb{R}^m$.

The discretization of $(\mathcal{P})$ reads as follows:

$$\left.\begin{array}{l}
\text{Find } (\boldsymbol{u}_h, \lambda_{h\nu}, \lambda_{ht}) \in \boldsymbol{V}_h \times \Lambda_{h\nu} \times \Lambda_{ht}(\lambda_{h\nu}) \text{ such that}\\
a(\boldsymbol{u}_h, \boldsymbol{v}_h) = L(\boldsymbol{v}_h) - \langle \lambda_{h\nu}, v_{h\nu} \rangle - \langle \lambda_{ht}, v_{ht} \rangle \quad \forall \boldsymbol{v}_h \in \boldsymbol{V}_h,\\
\langle \mu_{h\nu} - \lambda_{h\nu}, \mu_{h\nu} \rangle + \langle \mu_{ht} - \lambda_{ht}, \mu_{ht} \rangle \le 0 \quad \forall (\mu_{h\nu}, \mu_{ht}) \in \Lambda_{h\nu} \times \Lambda_{ht}(\lambda_{h\nu})
\end{array}\right\} (\mathcal{P})_h$$

or in the algebraic form:

$$\left.\begin{array}{l}
\text{Find } (\boldsymbol{u}, \boldsymbol{\lambda}_\nu, \boldsymbol{\lambda}_t) \in \mathbb{R}^n \times \boldsymbol{\Lambda}_\nu \times \boldsymbol{\Lambda}_t(\boldsymbol{\lambda}_\nu) \text{ such that}\\
\mathbb{K}\boldsymbol{u} = \boldsymbol{L} - \mathbb{N}^\top \boldsymbol{\lambda}_\nu - \mathbb{T}^\top \boldsymbol{\lambda}_t,\\
(\mathbb{N}\boldsymbol{u}, \boldsymbol{\mu}_\nu - \boldsymbol{\lambda}_\nu)_m + (\mathbb{T}\boldsymbol{u}, \boldsymbol{\mu}_t - \boldsymbol{\lambda}_t)_m \le 0 \quad \forall (\boldsymbol{\mu}_\nu, \boldsymbol{\mu}_t) \in \boldsymbol{\Lambda}_\nu \times \boldsymbol{\Lambda}_t(\boldsymbol{\lambda}_\nu),
\end{array}\right\} (\boldsymbol{\mathcal{P}})$$

where $\mathbb{K}$ is the $(n \times n)$ stiffness matrix, $\boldsymbol{L} \in \mathbb{R}^n$ is the load vector, $\mathbb{N}$, $\mathbb{T}$ are $(m \times n)$ matrices representing the linear trace mappings $\gamma_\nu$ and $\gamma_t$ in $\boldsymbol{V}_h$.

Problem $(\boldsymbol{\mathcal{P}})$ can be also written in the form of a *generalized equation* (GE). Indeed, let $N_Q(y)$ denote the standard normal cone to a nonempty convex set $Q$ at $y \in Q$. Then $(\boldsymbol{\mathcal{P}})$ is equivalent to

$$\left.\begin{array}{l} \mathbb{K}\boldsymbol{u} = \boldsymbol{L} - \mathbb{N}^\top \boldsymbol{\lambda}_\nu - \mathbb{T}^\top \boldsymbol{\lambda}_t, \\ \mathbb{N}\boldsymbol{u} \in N_{\boldsymbol{\Lambda}_\nu}(\boldsymbol{\lambda}_\nu),\ \mathbb{T}\boldsymbol{u} \in N_{\boldsymbol{\Lambda}_t(\boldsymbol{\lambda}_\nu)}(\boldsymbol{\lambda}_t). \end{array}\right\} \qquad (\boldsymbol{\mathcal{P}})_{GE}$$

This formulation enables us to prove the existence of local Lipschitz continuous branches of solutions to $(\boldsymbol{\mathcal{P}})$ which are parametrized by the coefficient of friction $\mathcal{F}$.

There is yet another equivalent formulation of $(\boldsymbol{\mathcal{P}})$ leading to a system of *nonsmooth equations* (NE) in $\mathbb{R}^{n+2m}$. The inequality in $(\boldsymbol{\mathcal{P}})$ can be expressed by means of projections of $\mathbb{R}^m$ onto $\boldsymbol{\Lambda}_\nu$ and $\boldsymbol{\Lambda}_t(\boldsymbol{g})$. Since the constraints in $\boldsymbol{\Lambda}_\nu$ and $\boldsymbol{\Lambda}_t(\boldsymbol{g})$ are separated, the respective projections split into $m$ projections in $\mathbb{R}$. Thus the projection $\boldsymbol{P}_{\mathbb{R}^m_+}$ of $\mathbb{R}^m$ onto $\mathbb{R}^m_+$ is given by

$$\boldsymbol{P}_{\mathbb{R}^m_+}(\boldsymbol{x}) = (P_{\mathbb{R}_+}(x_1), \ldots, P_{\mathbb{R}_+}(x_m))^\top,\ \boldsymbol{x} = (x_1, \ldots, x_m)^\top \in \mathbb{R}^m,$$

where $P_{\mathbb{R}_+}(z) = \max\{0, z\}$, $z \in \mathbb{R}$. Analogously, the projection $\boldsymbol{P}_{[-\boldsymbol{g},\boldsymbol{g}]}$ of $\mathbb{R}^m$ onto $\mathcal{K} = [-g_1, g_1] \times \cdots \times [-g_m, g_m]$, $\boldsymbol{g} = (g_1, \ldots, g_m) \geq \boldsymbol{0}$ is given by

$$\boldsymbol{P}_{[-\boldsymbol{g},\boldsymbol{g}]}(\boldsymbol{x}) = (P_{[-g_1,g_1]}(x_1), \ldots, P_{[-g_m,g_m]}(x_m))^\top,\ \boldsymbol{x} = (x_1, \ldots, x_m)^\top \in \mathbb{R}^m,$$

where $P_{[-y,y]} : \mathbb{R} \mapsto [-y, y]$, $P_{[-y,y]}(z) = \max\{0, z + y\} - \max\{0, z - y\} - y$, $\forall y \geq 0$ and $z \in \mathbb{R}$. It is easy to verify that the inequality in $(\boldsymbol{\mathcal{P}})$ can be equivalently written as

$$\boldsymbol{\lambda}_\nu - \boldsymbol{P}_{\mathbb{R}^m_+}(\boldsymbol{\lambda}_\nu + \rho\mathbb{N}\boldsymbol{u}) = \boldsymbol{0} \quad \text{and} \quad \boldsymbol{\lambda}_t - \boldsymbol{P}_{[-\boldsymbol{\mathcal{F}}\odot\boldsymbol{\lambda}_\nu, \boldsymbol{\mathcal{F}}\odot\boldsymbol{\lambda}_\nu]}(\boldsymbol{\lambda}_t + \rho\mathbb{T}\boldsymbol{u}) = \boldsymbol{0},$$

where $\rho > 0$ is arbitrary but fixed. The resulting system of nonsmooth equations reads as follows:

$$\left.\begin{array}{l} \text{Find } \boldsymbol{y}^* := (\boldsymbol{u}, \boldsymbol{\lambda}_\nu, \boldsymbol{\lambda}_t) \in \mathbb{R}^n \times \mathbb{R}^m \times \mathbb{R}^m \text{ such that} \\ \boldsymbol{G}(\boldsymbol{y}^*) := \left( \begin{array}{l} \mathbb{K}\boldsymbol{u} - \boldsymbol{L} + \mathbb{N}^\top \boldsymbol{\lambda}_\nu + \mathbb{T}^\top \boldsymbol{\lambda}_t \\ \boldsymbol{\lambda}_\nu - P_{\mathbb{R}^m_+}(\boldsymbol{\lambda}_\nu + \rho\mathbb{N}\boldsymbol{u}) \\ \boldsymbol{\lambda}_t - P_{[-\boldsymbol{\mathcal{F}}\odot\boldsymbol{\lambda}_\nu, \boldsymbol{\mathcal{F}}\odot\boldsymbol{\lambda}_\nu]}(\boldsymbol{\lambda}_t + \rho\mathbb{T}\boldsymbol{u}) \end{array} \right) = \boldsymbol{0} \end{array}\right\} \qquad (\boldsymbol{\mathcal{P}})_{NE}$$

The mapping $\boldsymbol{G} : \mathbb{R}^{n+2m} \mapsto \mathbb{R}^{n+2m}$ is continuous and *piecewise affine* (see [22, 1]). Problem $(\boldsymbol{\mathcal{P}})_{NE}$ is a basis for the application of the semismooth Newton method which is the main tool in the nonsmooth path-following algorithm presented in Section 5.

## 3. Existence of locally unique solutions to $(\boldsymbol{\mathcal{P}})$

The aim of this section is to give an overview of results on the existence and possible uniqueness of solutions to $(\boldsymbol{\mathcal{P}})$ and the existence of local Lipschitz continuous branches of solutions with respect to the coefficient $\boldsymbol{\mathcal{F}} \in \mathbb{R}^m_{++}$ and the load vector $\boldsymbol{L}$ [10, 18].

It is easy to show that the matrices $\mathbb{K}$, $\mathbb{N}$, $\mathbb{T}$ in $(\boldsymbol{\mathcal{P}})$ have the following properties:

$$\mathbb{K} \text{ is symmetric and positive definite,} \tag{10}$$

$$\mathbb{N}^\top \boldsymbol{\mu}_\nu + \mathbb{T}^\top \boldsymbol{\mu}_t = \mathbf{0} \Longleftrightarrow (\boldsymbol{\mu}_\nu, \boldsymbol{\mu}_t) = \mathbf{0}, \tag{11}$$

or equivalently

$$\exists \beta > 0 : \quad \sup_{\substack{\boldsymbol{v} \in \mathbb{R}^m \\ \boldsymbol{v} \neq \mathbf{0}}} \frac{(\boldsymbol{\mu}_\nu, \mathbb{N}\boldsymbol{v})_m + (\boldsymbol{\mu}_t, \mathbb{T}\boldsymbol{v})_m}{\|\boldsymbol{v}\|_n} \geq \beta \|(\boldsymbol{\mu}_\nu, \boldsymbol{\mu}_t)\|_{2m} \quad \forall (\boldsymbol{\mu}_\nu, \boldsymbol{\mu}_t) \in \mathbb{R}^m \times \mathbb{R}^m. \tag{12}$$

To emphasize the fact that $\boldsymbol{\mathcal{F}} \in \mathbb{R}^m_{++}$ and $\boldsymbol{L} \in \mathbb{R}^n$ will be used as parameters in $(\boldsymbol{\mathcal{P}})$, we shall write $(\boldsymbol{\mathcal{P}}(\boldsymbol{\mathcal{F}}, \boldsymbol{L}))$ in what follows.

Denote by $\boldsymbol{S}_{\boldsymbol{\mathcal{F}},\boldsymbol{L}} \subset \mathbb{R}^{n+2m}$ the solution set of $(\boldsymbol{\mathcal{P}}(\boldsymbol{\mathcal{F}}, \boldsymbol{L}))$, $(\boldsymbol{\mathcal{F}}, \boldsymbol{L}) \in \mathbb{R}^m_{++} \times \mathbb{R}^n$, i.e.

$$\boldsymbol{y} \in \boldsymbol{S}_{\boldsymbol{\mathcal{F}},\boldsymbol{L}} \Longleftrightarrow \boldsymbol{y} = (\boldsymbol{u}, \boldsymbol{\lambda}_\nu, \boldsymbol{\lambda}_t) \text{ solves } (\boldsymbol{\mathcal{P}}(\boldsymbol{\mathcal{F}}, \boldsymbol{L})).$$

From (10) and (11) it follows that

*(i)* $\boldsymbol{S}_{\boldsymbol{\mathcal{F}},\boldsymbol{L}} \neq \emptyset \quad \forall (\boldsymbol{\mathcal{F}}, \boldsymbol{L}) \in \mathbb{R}^m_{++} \times \in \mathbb{R}^n$;

*(ii)* for any $R > 0$ the set $\bigcup_{\boldsymbol{L} \in B_R(\mathbf{0})} \boldsymbol{S}_{\boldsymbol{\mathcal{F}},\boldsymbol{L}}$ is bounded uniformly with respect to $\boldsymbol{\mathcal{F}} \in \mathbb{R}^m_{++}$:

$$\forall R > 0 \; \exists c_R > 0 : \|\boldsymbol{y}\|_{n+2m} \leq c_R \quad \forall \boldsymbol{y} \in \boldsymbol{S}_{\boldsymbol{\mathcal{F}},\boldsymbol{L}} \quad \forall \boldsymbol{L} \in B_R(\mathbf{0}) \quad \forall \boldsymbol{\mathcal{F}} \in \mathbb{R}^m_{++},$$

where $\|\boldsymbol{y}\|_{n+2m} := \|\boldsymbol{u}\|_n + \|(\boldsymbol{\lambda}_\nu, \boldsymbol{\lambda}_t)\|_{2m}$ and $B_R(\mathbf{0})$ is the ball of radius $R$ and center at $\mathbf{0}$. In addition, $c_R \to \infty$ if $R \to \infty$;

*(iii)* there exists a critical value $\mathcal{F}_{\text{crit}} > 0$ such that $(\boldsymbol{\mathcal{P}}(\boldsymbol{\mathcal{F}}, \boldsymbol{L}))$ has a unique solution for any $\boldsymbol{\mathcal{F}} \in \mathcal{A}$ and $\boldsymbol{L} \in \mathbb{R}^n$, where

$$\mathcal{A} = \{\boldsymbol{\mathcal{F}} \in \mathbb{R}^m_{++} | \; \|\boldsymbol{\mathcal{F}}\|_{m,\infty} \leq \mathcal{F}_{\text{crit}}\}.$$

**Remark 2.** Point out that *(iii)* is only sufficient but not necessary condition guaranteeing the uniqueness of the solution to $(\boldsymbol{\mathcal{P}}(\boldsymbol{\mathcal{F}}, \boldsymbol{L}))$. The critical value $\mathcal{F}_{\text{crit}} > 0$ depends on $\beta$ from (12) and the condition number $\kappa(\mathbb{K}) = \lambda_{\max}(\mathbb{K})/\lambda_{\min}(\mathbb{K})$, where $\lambda_{\min}(\mathbb{K})$, $\lambda_{\max}(\mathbb{K})$ is the minimal and maximal eigenvalue of $\mathbb{K}$, respectively. Consequently, $\mathcal{F}_{\text{crit}}$ depends on the size of the problem, i.e. on $n$ and $m$. It is known that $\mathcal{F}_{\text{crit}} \to 0+$ if $n, m \to \infty$. This means that the unicity of a solution may be lost when passing to finer meshes. Upper bounds for $\mathcal{F}_{\text{crit}}$ in terms of the mesh norms have been derived in [8] and for 3D problems with orthotropic friction in [12].

Let $(\boldsymbol{\mathcal{F}}_0, \boldsymbol{L}_0) \in \mathbb{R}^m_{++} \times \mathbb{R}^n$ be an arbitrary but fixed reference point. We denote by $\mathscr{S}_{\boldsymbol{\mathcal{F}}_0} : \mathbb{R}^n \mapsto \mathbb{R}^{n+2m}$, $\mathscr{S}_{\boldsymbol{L}_0} : \mathbb{R}^m_{++} \mapsto \mathbb{R}^{n+2m}$ generally multivalued mappings defined by

$$\mathscr{S}_{\boldsymbol{\mathcal{F}}_0} : \boldsymbol{L} \mapsto \mathscr{S}_{\boldsymbol{\mathcal{F}}_0}(\boldsymbol{L}) \in \boldsymbol{S}_{\boldsymbol{\mathcal{F}}_0, \boldsymbol{L}}, \quad \boldsymbol{L} \in \mathbb{R}^n$$

and

$$\mathscr{S}_{\boldsymbol{L}_0} : \boldsymbol{\mathcal{F}} \mapsto \mathscr{S}_{\boldsymbol{L}_0}(\boldsymbol{\mathcal{F}}) \in \boldsymbol{S}_{\boldsymbol{\mathcal{F}}, \boldsymbol{L}_0}, \quad \boldsymbol{\mathcal{F}} \in \mathbb{R}^m_{++},$$

respectively.

From *(iii)* it follows that $\mathscr{S}_{\boldsymbol{\mathcal{F}}_0}$ is single valued on $\mathbb{R}^n$ for any $\boldsymbol{\mathcal{F}}_0 \in \mathcal{A}$ and the restriction $\mathscr{S}_{\boldsymbol{L}_0|_{\mathcal{A}}}$ is single valued on $\mathcal{A}$ for any $\boldsymbol{L}_0 \in \mathbb{R}^n$. Moreover, one can directly show ([12]) that $\mathscr{S}_{\boldsymbol{\mathcal{F}}_0}$, $\boldsymbol{\mathcal{F}}_0 \in \mathcal{A}$ is Lipschitz continuous in $\mathbb{R}^n$ and $\mathscr{S}_{\boldsymbol{L}_0|_{\mathcal{A}}}$ is locally Lipschitz continuous in $\mathcal{A}$.

The situation for $\boldsymbol{\mathcal{F}} \notin \mathcal{A}$ is more involved since the uniqueness of a solution to $(\boldsymbol{\mathcal{P}})$ is not guaranteed. However, one can ask if there exist locally unique solutions in a vicinity of a reference point which are Lipschitz continuous functions of $\boldsymbol{\mathcal{F}}$ and $\boldsymbol{L}$. Conditions ensuring the existence of local Lipschitz continuous branches of $\mathscr{S}_{\boldsymbol{L}_0}$ are formulated in the following generalization of the classical implicit function theorem [20].

**Theorem 1.** *Let $(\boldsymbol{\mathcal{F}}_0, \boldsymbol{L}_0) \in \mathbb{R}^m_{++} \times \mathbb{R}^n$ be given and let $\boldsymbol{y}_0 \in \boldsymbol{S}_{\boldsymbol{\mathcal{F}}_0, \boldsymbol{L}_0}$. Suppose that $\mathscr{S}_{\boldsymbol{\mathcal{F}}_0}$ has a local Lipschitz continuous branch containing $\boldsymbol{y}_0$, i.e. there exist open sets $\boldsymbol{U} \subset \mathbb{R}^n$, $\boldsymbol{Y} \subset \mathbb{R}^{n+2m}$ such that $(\boldsymbol{L}_0, \boldsymbol{y}_0) \in \boldsymbol{U} \times \boldsymbol{Y}$ and a single valued Lipschitz continuous function $\sigma_{\boldsymbol{\mathcal{F}}_0} : \boldsymbol{U} \mapsto \boldsymbol{Y}$ satisfying:*

$$\sigma_{\boldsymbol{\mathcal{F}}_0}(\boldsymbol{L}_0) = \boldsymbol{y}_0 \quad \textit{and} \quad \sigma_{\boldsymbol{\mathcal{F}}_0}(\boldsymbol{L}) = \mathscr{S}_{\boldsymbol{\mathcal{F}}_0}(\boldsymbol{L}) \cap \boldsymbol{Y} \quad \forall \boldsymbol{L} \in \boldsymbol{U}.$$

*Then there exist: open sets $\widehat{\boldsymbol{U}} \subset \mathbb{R}^m_{++}$ and $\widehat{\boldsymbol{Y}} \subset \mathbb{R}^{n+2m}$ such that $(\boldsymbol{\mathcal{F}}_0, \boldsymbol{y}_0) \in \widehat{\boldsymbol{U}} \times \widehat{\boldsymbol{Y}}$ and a single valued Lipschitz continuous function $\sigma_{\boldsymbol{L}_0} : \widehat{\boldsymbol{U}} \mapsto \widehat{\boldsymbol{Y}}$ satisfying:*

$$\sigma_{\boldsymbol{L}_0}(\boldsymbol{\mathcal{F}}_0) = \boldsymbol{y}_0 \quad \textit{and} \quad \sigma_{\boldsymbol{L}_0}(\boldsymbol{\mathcal{F}}) = \mathscr{S}_{\boldsymbol{L}_0}(\boldsymbol{\mathcal{F}}) \cap \widehat{\boldsymbol{Y}} \quad \forall \boldsymbol{\mathcal{F}} \in \widehat{\boldsymbol{U}}.$$

From this theorem it follows that to prove the existence of local Lipschitz continuous branches of $\mathscr{S}_{\boldsymbol{L}}$ one has to establish the existence of local Lipschitz continuous branches of $\mathscr{S}_{\boldsymbol{\mathcal{F}}}$ in a vicinity $\boldsymbol{y} \in \mathscr{S}_{\boldsymbol{\mathcal{F}}}(\boldsymbol{L})$ keeping $\boldsymbol{\mathcal{F}}$ fixed. But the later problem is considerably easier since $\mathscr{S}_{\boldsymbol{\mathcal{F}}}$ is piecewise affine in $\mathbb{R}^n$. It has been shown in [18] that the existence of such branches is not guaranteed in a vicinity of $\boldsymbol{y}$ only for load vectors $\boldsymbol{L} \in \mathbb{R}^n$ which belong to the union of subspaces of dimension strictly less than $n$.

## 4. Active set strategy algorithm for solving $(\mathcal{P})_{NE}$

This section deals with the active set strategy implementation of the semismooth Newton method for solving $(\mathcal{P})_{NE}$. If $\boldsymbol{G}$ was smooth enough, the $k$-th step of the classical Newton method would read as follows:

$$\mathbb{J}(\boldsymbol{y}^{(k-1)})\boldsymbol{y}^{(k)} = \mathbb{J}(\boldsymbol{y}^{(k-1)})\boldsymbol{y}^{(k-1)} - \boldsymbol{G}(\boldsymbol{y}^{(k-1)}), \quad k = 1, 2, \ldots, \tag{13}$$

where $\mathbb{J} : \mathbb{R}^{n+2m} \mapsto \mathbb{R}^{(n+2m)\times(n+2m)}$ and $\mathbb{J}(\boldsymbol{y})$, $\boldsymbol{y} \in \mathbb{R}^{n+2m}$, is the Jacobian of $\boldsymbol{G}$ at $\boldsymbol{y}$. If $\mathbb{J}$ is non-differentiable at some points, we use the active set strategy described in what follows.

Let $\mathcal{M} = \{1, 2, \ldots, m\}$, where $m$ is the number of contact nodes. The *inactive* sets $\mathcal{I}_\nu := \mathcal{I}_\nu(\boldsymbol{y})$, $\mathcal{I}_t^+ := \mathcal{I}_t^+(\boldsymbol{y})$, and $\mathcal{I}_t^- := \mathcal{I}_t^-(\boldsymbol{y})$ at $\boldsymbol{y} = (\boldsymbol{v}, \boldsymbol{\mu}_\nu, \boldsymbol{\mu}_t) \in \mathbb{R}^{n+2m}$ are defined by

$$\begin{aligned}
\mathcal{I}_\nu &= \{i \in \mathcal{M} : (\boldsymbol{\mu}_\nu + \rho\mathbb{N}\boldsymbol{v})_i < 0\},\\
\mathcal{I}_t^+ &= \{i \in \mathcal{M} : (\boldsymbol{\mu}_t + \rho\mathbb{T}\boldsymbol{v})_i - \mathcal{F}_i P_{\mathbb{R}_+}((\boldsymbol{\mu}_\nu + \rho\mathbb{N}\boldsymbol{v})_i) > 0\},\\
\mathcal{I}_t^- &= \{i \in \mathcal{M} : (\boldsymbol{\mu}_t + \rho\mathbb{T}\boldsymbol{v})_i + \mathcal{F}_i P_{\mathbb{R}_+}((\boldsymbol{\mu}_\nu + \rho\mathbb{N}\boldsymbol{v})_i) < 0\},
\end{aligned}$$

while the *active* sets are their complements: $\mathcal{A}_\nu := \mathcal{A}_\nu(\boldsymbol{y}) = \mathcal{M} \setminus \mathcal{I}_\nu$, $\mathcal{A}_t := \mathcal{A}_t(\boldsymbol{y}) = \mathcal{M} \setminus (\mathcal{I}_t^+ \cup \mathcal{I}_t^-)$. Denote $\mathcal{I} := \mathcal{I}(\boldsymbol{y}) = \{\mathcal{I}_\nu, \mathcal{I}_t^+, \mathcal{I}_t^-\}$, which gives the complete information on the active and inactive sets at $\boldsymbol{y}$. For a subset $\mathcal{S} \subseteq \mathcal{M}$ we introduce the indicator matrix $\mathbb{D}_{\mathcal{S}} = diag(s_1, \ldots, s_m) \in \mathbb{R}^{m\times m}$ with $s_i = 1$, if $i \in \mathcal{S}$, and $s_i = 0$, if $i \notin \mathcal{S}$. Taking into account this decomposition of $\mathcal{M}$, the function $\boldsymbol{G}$ in $(\mathcal{P})_{NE}$ can be written as follows:

$$\boldsymbol{G}(\boldsymbol{y}) = \begin{pmatrix} \mathbb{K}\boldsymbol{v} - \boldsymbol{L} + \mathbb{N}^\top\boldsymbol{\mu}_\nu + \mathbb{T}^\top\boldsymbol{\mu}_t \\ \boldsymbol{\mu}_\nu - \mathbb{D}_{\mathcal{A}_\nu}(\boldsymbol{\mu}_\nu + \rho\mathbb{N}\boldsymbol{v}) \\ \boldsymbol{\mu}_t - \mathbb{D}_{\mathcal{A}_t}(\boldsymbol{\mu}_t + \rho\mathbb{T}\boldsymbol{v}) + (\mathbb{D}_{\mathcal{I}_t^-} - \mathbb{D}_{\mathcal{I}_t^+})\mathbb{D}_{\mathcal{A}_\nu}\boldsymbol{\mathcal{F}} \odot (\boldsymbol{\mu}_\nu + \rho\mathbb{N}\boldsymbol{v}) \end{pmatrix} \tag{14}$$

for every $\boldsymbol{y} \in \mathbb{R}^{n+2m}$. This expression of $\boldsymbol{G}$ and its Jacobian lead to the following form of the $k$-th iterative step (13):

$$\begin{pmatrix} \mathbb{K} & \mathbb{N}^\top & \mathbb{T}^\top \\ -\rho\mathbb{D}_{\mathcal{A}_\nu}\mathbb{N} & \mathbb{D}_{\mathcal{I}_\nu} & \mathbb{O} \\ -\rho\mathbb{D}_{\mathcal{A}_t}\mathbb{T} & (\mathbb{D}_{\mathcal{I}_t^-} - \mathbb{D}_{\mathcal{I}_t^+})\mathbb{D}_{\mathcal{A}_\nu}\mathbb{F} & \mathbb{D}_{\mathcal{I}_t^+ \cup \mathcal{I}_t^-} \end{pmatrix} \boldsymbol{y}^{(k)} = \begin{pmatrix} \boldsymbol{L} \\ \boldsymbol{0} \\ \boldsymbol{0} \end{pmatrix}, \tag{15}$$

where $\mathbb{F} = diag(\boldsymbol{\mathcal{F}})$ and $\mathcal{I} := \mathcal{I}(\boldsymbol{y}^{(k-1)})$. It is easily seen that the solution $\boldsymbol{y}^{(k)} = (\boldsymbol{u}^{(k)}, \boldsymbol{\lambda}_\nu^{(k)}, \boldsymbol{\lambda}_t^{(k)})$ to (15) satisfies at the contact nodes:

$$(\mathbb{N}\boldsymbol{u}^{(k)})_i = 0, \ i \in \mathcal{A}_\nu, \tag{16}$$
$$(\boldsymbol{\lambda}_\nu^{(k)})_i = 0, \ i \in \mathcal{I}_\nu, \tag{17}$$
$$(\mathbb{T}\boldsymbol{u}^{(k)})_i = 0, \ i \in \mathcal{A}_t, \tag{18}$$
$$(\boldsymbol{\lambda}_t^{(k)})_i + \mathcal{F}_i(\boldsymbol{\lambda}_\nu^{(k)})_i(\mathbb{D}_{\mathcal{A}_\nu})_{ii} = 0, \ i \in \mathcal{I}_t^-, \tag{19}$$
$$(\boldsymbol{\lambda}_t^{(k)})_i - \mathcal{F}_i(\boldsymbol{\lambda}_\nu^{(k)})_i(\mathbb{D}_{\mathcal{A}_\nu})_{ii} = 0, \ i \in \mathcal{I}_t^+. \tag{20}$$

As the active and inactive sets are disjoint, the contact nodes can be split into the nodes with the prescribed Dirichlet ((16), (18)) and the Neumann ((17), (19), (20)) conditions. Solutions to (15) with $\mathcal{I} := \mathcal{I}(\boldsymbol{y})$, $\boldsymbol{y} \in \mathbb{R}^{n+2m}$ will be denoted in a symbolic way as $DirNeu(\mathcal{I})$ in what it follows. We arrive at the following active set strategy implementation of (13).

ALGORITHM *SSNM* (SemiSmooth Newton Method) Given $\boldsymbol{y}^{(0)} \in \mathbb{R}^{n+2m}$, $\varepsilon > 0$, and $k_{max} \geq 2$. Set $k := 1$;

*(i)* Define the active and inactive sets: $\mathcal{I} := \mathcal{I}(\boldsymbol{y}^{(k-1)})$;

*(ii)* Solve the linear system (15): $\boldsymbol{y}^{(k)} = DirNeu(\mathcal{I})$;

*(iii)* Stop, if $\|\boldsymbol{y}^{(k)} - \boldsymbol{y}^{(k-1)}\|/\|\boldsymbol{y}^{(k)}\| \leq \varepsilon$ or $k = k_{max}$, else set $k := k + 1$ and go to step *(i)*.

The numerical solution to $(\boldsymbol{\mathcal{P}})_{NE}$ computed by this algorithm will be denoted by

$$\boldsymbol{y}^{(\bar{k})} = SSNM(\boldsymbol{y}^{(0)}),$$

where $\bar{k}$ stands for the last iteration, for which the stopping criterion in *(iii)* is achieved. In our computations we use $\varepsilon = 10^{-6}$ and $k_{max} = 15$. These values however are not important from the point of view of the continuation algorithm.

Next, we will always assume that the following assumption is satisfied.

**Assumption 1.** *The Jacobian $\mathbb{J}(\boldsymbol{y}^*)$, where $\boldsymbol{y}^*$ is a solution to $(\boldsymbol{\mathcal{P}})_{NE}$ is non-singular for any decomposition of $\mathcal{M}$ into the active and inactive sets at $\boldsymbol{y}^*$.*

The following result is well-known (see [3, 15]).

**Theorem 2.** *Let Assumption 1 be satisfied. If the initial iteration $\boldsymbol{y}^{(0)} \in \mathbb{R}^{n+2m}$ is sufficiently close to the solution $\boldsymbol{y}^*$ of $(\boldsymbol{\mathcal{P}})_{NE}$, the sequence $\{\boldsymbol{y}^{(k)}\}$ generated by* Algorithm *SSNM converges superlinearly to $\boldsymbol{y}^*$.*

The following two lemmas play the key role in the predictor-corrector approach used in the continuation algorithm which is presented in the next section.

**Lemma 1.** *Let Assumption 1 be satisfied, $\boldsymbol{y}^*$ be the solution to $(\boldsymbol{\mathcal{P}})_{NE}$ and set $\mathcal{I}^* := \mathcal{I}(\boldsymbol{y}^*)$. Then $\boldsymbol{y}^* = DirNeu(\mathcal{I}^*)$.*

*Proof* Denote $\bar{\boldsymbol{y}} = DirNeu(\mathcal{I}^*)$. From (13) for $\boldsymbol{y}^{(k-1)} = \boldsymbol{y}^*$ we have

$$\mathbb{J}(\boldsymbol{y}^*)\bar{\boldsymbol{y}} = \mathbb{J}(\boldsymbol{y}^*)\boldsymbol{y}^* - \boldsymbol{G}(\boldsymbol{y}^*).$$

As $\boldsymbol{G}(\boldsymbol{y}^*) = \boldsymbol{0}$ and $\mathbb{J}(\boldsymbol{y}^*)$ is non-singular, we get $\bar{\boldsymbol{y}} = \boldsymbol{y}^*$. □

**Lemma 2.** *Let Assumption 1 be satisfied, $\boldsymbol{y}^*$ be the solution to $(\boldsymbol{\mathcal{P}})_{NE}$ and $\boldsymbol{y}^{(0)} = \boldsymbol{y}^*$. Then $\boldsymbol{y}^{(1)} = \boldsymbol{y}^*$, where $\boldsymbol{y}^{(1)} = SSNM(\boldsymbol{y}^{(0)})$.*

*Proof* It is analogous to the one of Lemma 1. Now for $\boldsymbol{y}^{(0)} = \boldsymbol{y}^*$ we get from (13):

$$\mathbb{J}(\boldsymbol{y}^*)\boldsymbol{y}^{(1)} = \mathbb{J}(\boldsymbol{y}^*)\boldsymbol{y}^* - \boldsymbol{G}(\boldsymbol{y}^*).$$

Thus $\boldsymbol{y}^{(1)} = \boldsymbol{y}^*$. □

From these lemmas, one can decide whether the active and inactive sets given by some $\bar{\mathcal{I}}$ define a solution to $(\boldsymbol{\mathcal{P}})_{NE}$. We proceed as follows. First, we predict $\bar{\boldsymbol{y}}$ by solving the linear system (15):

$$\text{Predictor:} \quad \bar{\boldsymbol{y}} = DirNeu(\bar{\mathcal{I}}).$$

To confirm whether $\bar{\boldsymbol{y}}$ is the solution to $(\boldsymbol{\mathcal{P}})_{NE}$, we use the corrector step:

$$\text{Corrector:} \quad \boldsymbol{y}^{(\bar{k})} = SSNM(\bar{\boldsymbol{y}}).$$

If $\bar{k} = 1$, then $\boldsymbol{y}^* = \bar{\boldsymbol{y}} = \boldsymbol{y}^{(1)}$, as follows from Lemma 1 and 2, and $\bar{\mathcal{I}} = \mathcal{I}(\boldsymbol{y}^*)$. Otherwise $\bar{\boldsymbol{y}}$ does not solve $(\boldsymbol{\mathcal{P}})_{NE}$ and $\bar{\mathcal{I}} \neq \mathcal{I}(\boldsymbol{y}^*)$.

## 5. Nonsmooth continuation algorithm

Next we shall assume that problem $(\boldsymbol{\mathcal{P}})_{NE}$ is parametrized by means of a scalar $\alpha \in \mathbb{R}$. To emphasize this fact, we will use the following notation: $\boldsymbol{y}^*(\alpha)$ for a solution to $(\boldsymbol{\mathcal{P}}(\alpha))_{NE}$, $\boldsymbol{y}(\alpha) = DirNeu(\mathcal{I}, \alpha)$, and $\boldsymbol{y}^{(\bar{k})} = SSNM(\boldsymbol{y}^{(0)}, \alpha)$, respectively.

We seek the *solution path* that is a curve $\mathcal{C}$ in $\mathbb{R} \times \mathbb{R}^{n+2m}$ defined by

$$\mathcal{C} = \{(\alpha, \boldsymbol{y}^*(\alpha)) \in \mathbb{R} \times \mathbb{R}^{n+2m}\}$$

We assume that either the load vector $\boldsymbol{L}$ or the coefficient of friction $\boldsymbol{\mathcal{F}}$ depend on $\alpha$ and that the mappings $\alpha \mapsto \boldsymbol{L}(\alpha)$, $\boldsymbol{\mathcal{F}}(\alpha)$ are affine. Although the definition of $\mathcal{C}$ is the same for both cases, the typical character of $\mathcal{C}$ is different, see Figure 1. If the load vector $\boldsymbol{L}$ depends on $\alpha$ then $\mathcal{C}$ is piecewise affine. On the other hand, if the coefficient of friction $\boldsymbol{\mathcal{F}}$ is parameter dependent then $\mathcal{C}$ is piecewise smooth (not necessarily piecewise affine). Further, the solution path $\mathcal{C}$ may consist of non-connected continuous *branches*. This fact follows from Theorem 1 (also see [10, 16], where simple models with parameter dependent coefficient of friction and one or two finite element nodes were analyzed). Any branch of $\mathcal{C}$ may contain nonsmooth points $Q := (\alpha, \boldsymbol{y}^*(\alpha)) \in \mathcal{C}$ of two types:

*(a)* $Q$ is the *transversal transition* point, if

$$\forall R > 0\ \exists \gamma > 0\ \forall \bar{\alpha} \in (\alpha - \gamma, \alpha + \gamma)\ \exists \bar{Q} := (\bar{\alpha}, \boldsymbol{y}^*(\bar{\alpha}))\ :\ \bar{Q} \in \mathcal{C} \cap B_R(Q);$$

*(b)* $Q$ is the *right turning transition* point, if

$$\forall R > 0\ \exists \gamma > 0\ \forall \bar{\alpha} \in (\alpha, \alpha + \gamma)\ \exists \bar{Q}_1 := (\bar{\alpha}, \boldsymbol{y}_1^*(\bar{\alpha})) \& \bar{Q}_2 := (\bar{\alpha}, \boldsymbol{y}_2^*(\bar{\alpha}))\ :$$

$$\bar{Q}_1 \neq \bar{Q}_2\ \&\ \bar{Q}_1, \bar{Q}_2 \in \mathcal{C} \cap B_R(Q);$$

where $B_R(Q)$ is the ball of radius $R$ and center at $Q$. The *left turning transition* point is defined analogously; see Figure 1. Nonsmooth points on $\mathcal{C}$ correspond to those $\bar{\alpha}$ such that at least one inactive constraint defining $\mathcal{I}(\boldsymbol{y}^*(\bar{\alpha}))$ changes to the active one. The segment of $\mathcal{C}$ between two transition points is called a *piece*. Each piece is smooth (or even affine). Assumption 1 excludes other types of nonsmooth points arising, e.g., when the problem $(\boldsymbol{\mathcal{P}}(\alpha))_{NE}$ has a continuum of solutions for some $\alpha$ [22], i.e., the branch contains a vertical segment.

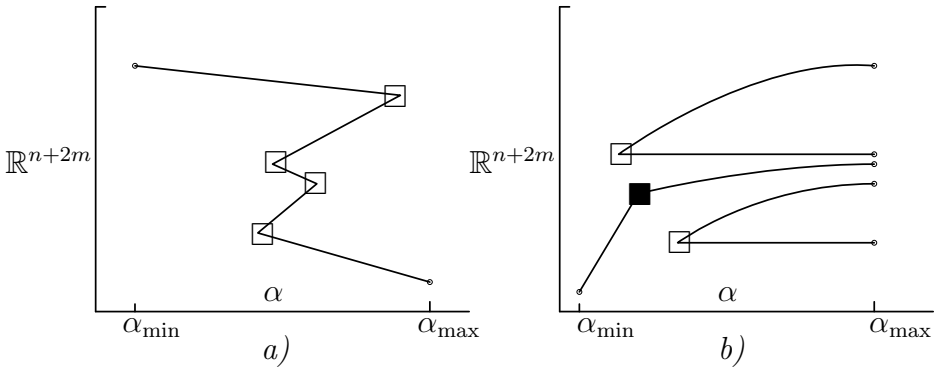


Figure 1: *a)* $\boldsymbol{L} := \boldsymbol{L}(\alpha)$, four turning transition points (□), five pieces; *b)* $\boldsymbol{\mathcal{F}} := \boldsymbol{\mathcal{F}}(\alpha)$, one transversal transition point (■), two turning transition points (□), three branches each of them with two pieces.

The continuation algorithm along one branch generates a sequence of points lying on this branch. The algorithm consists of two parts: *(i)* an *adaptive* continuation along a piece. It enables to approach a nonsmooth point on $\mathcal{C}$ with a high accuracy; *(ii)* a *detection* of a new smooth piece from a point sufficiently close to a nonsmooth one. To find further branches for the model with parameter dependent $\boldsymbol{\mathcal{F}}$, we use the auxiliary model with parameter dependent $\boldsymbol{L}$ starting from an appropriate point. This makes it possible to find multiple solutions. Then starting from these multiple solutions, one can perform the continuation by $\boldsymbol{\mathcal{F}}$ to detect another branch of $\mathcal{C}$. In the rest of this section we show how to apply the predictor-corrector strategy to realize the these steps.

*5.1. Continuation along a smooth piece*

Let $\mathcal{C}_{piece} \subset \mathcal{C}$ be a smooth piece of $\mathcal{C}$. The continuation along $\mathcal{C}_{piece}$ is based on a one-step recurrence:

$$(\alpha_{i-1}, \boldsymbol{y}^*(\alpha_{i-1})) \in \mathcal{C}_{piece} \to (\alpha_i, \boldsymbol{y}^*(\alpha_i)) \in \mathcal{C}_{piece},$$

where $\alpha_{i-1}$ and $\boldsymbol{y}^*(\alpha_{i-1})$ are known. The continuation uses the fact that the active and inactive sets remain the same along $\mathcal{C}_{piece}$. First, we predict $\bar{\alpha} = \alpha_{i-1} + s\delta$, where $s$ is the *orientation* (1 or $-1$) of $\mathcal{C}_{piece}$ and $\delta$ is the *step-length*, $0 < \delta_{\min} \le \delta \le \delta_{\max}$. The orientations are determined by

$$s = \frac{\bar{\alpha} - \alpha_{i-1}}{|\bar{\alpha} - \alpha_{i-1}|}.$$

Then we apply the predictor-corrector technique to decide whether $\bar{\alpha}$ and the respective solution to $(\boldsymbol{\mathcal{P}}(\bar{\alpha}))_{NE}$ determine a new point on $\mathcal{C}_{piece}$ or not. To be able to approach a nonsmooth point of $\mathcal{C}_{piece}$ with a high accuracy, we use the adaptive step-length strategy controled by the *shortening* rate $c_s$, $0 < c_s < 1$ and the *prolongation* rate $c_p$, $1 < c_p$. The algorithm reads as follows:

ALGORITHM *PC* (Predictor-Corrector)

*(i)* Define: $\bar{\alpha} = \alpha_{i-1} + s\delta$, $\bar{\mathcal{I}} := \mathcal{I}(\boldsymbol{y}^*(\alpha_{i-1}))$;

*(ii)* Predictor-corrector: $\boldsymbol{y}^{(0)} = \mathit{DirNeu}(\bar{\mathcal{I}}, \bar{\alpha})$, $\boldsymbol{y}^{(\bar{k})} = \mathit{SSNM}(\boldsymbol{y}^{(0)}, \bar{\alpha})$;

*(iii)* Decision:

`if` $\bar{k} = 1,\ \alpha_i := \bar{\alpha},\ \boldsymbol{y}^*(\alpha_i) := \boldsymbol{y}^{(1)},\ \delta := \min\{c_p\delta, \delta_{\max}\}$, `return`

`elseif` $\delta = \delta_{\min}$, `fail`

`else` $\delta := \max\{c_s\delta, \delta_{\min}\}$, `go to step` *(i)*.

If $\bar{k} = 1$, the algorithm returns the new point $(\alpha_i, \boldsymbol{y}^*(\alpha_i)) \in \mathcal{C}_{piece}$ with $\mathcal{I}(\boldsymbol{y}^*(\alpha_i)) = \mathcal{I}(\boldsymbol{y}^*(\alpha_{i-1}))$; see Figure 2 *a)*. Note that the orientation $s$ of $\mathcal{C}_{piece}$ is not changed. Then we apply ALGORITHM *PC* repeatedly with $i := i + 1$. In the case of the failure, the last accepted point is $(\alpha_{i-1}, \boldsymbol{y}^*(\alpha_{i-1})) \in \mathcal{C}_{piece}$; see Figure 2 *b)*. Moreover, if $\delta_{\min}$ is sufficiently small, this point is close to a nonsmooth point of $\mathcal{C}$.

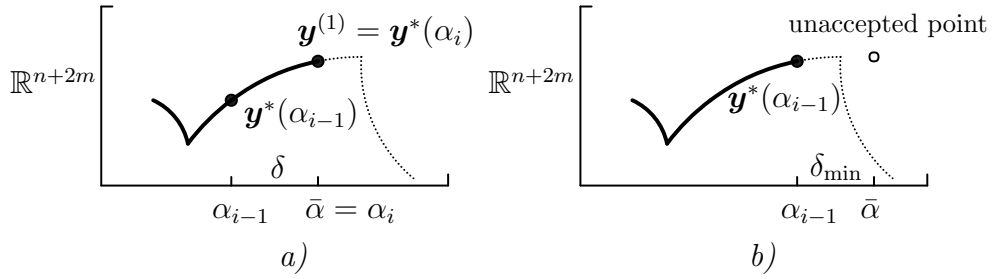


Figure 2: The result from the corrector is either accepted *(a)* or not *(b)*.

ALGORITHM *PC* can be characterized as a *tangent continuation* (see [4], Algorithm 4.25). The step-size control is inspired by [5].

*5.2. Detection of a new smooth piece*

Let $(\alpha_{i-1}, \boldsymbol{y}^*(\alpha_{i-1})) \in \mathcal{C}_{piece}$ be the last point computed by ALGORITHM *PC* ended by the failure with $\delta = \delta_{\min}$; see Figure 2 *b)* and Figure 3 *a)* and *b)*. Let $\bar{\alpha} = \alpha_{i-1} + s\delta_{\min}$. It follows from ALGORITHM *PC* that the active and

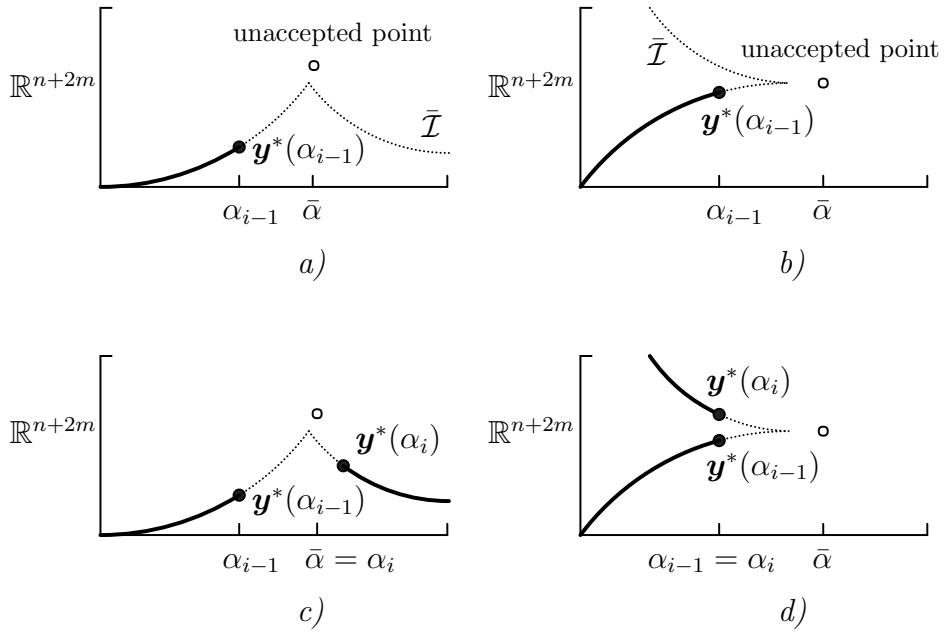


Figure 3: *a)* and *b)*: $\bar{\mathcal{I}}$ is the prediction of the active and inactive sets for $\mathcal{C}^{new}_{piece}$. *c)* and *d)*: the identification of $\mathcal{C}^{new}_{piece}$ after using the predictor-corrector technique; the transversal transition point with $s := s$ *(c)*; the left turning transition point with $s := -s$ *(d)*.

inactive sets at the solution $\boldsymbol{y}^*(\bar{\alpha})$ to $(\boldsymbol{\mathcal{P}}(\bar{\alpha}))_{NE}$ are not given by $\mathcal{I}(\boldsymbol{y}^*(\alpha_{i-1}))$. One can use $\bar{\alpha}$ to detect a new smooth piece $\mathcal{C}^{new}_{piece}$ belonging to the same branch of $\mathcal{C}$, but with different active and inactive sets. This is represented by the following one-step recurrence:

$$(\alpha_{i-1}, \boldsymbol{y}^*(\alpha_{i-1})) \in \mathcal{C}_{piece} \rightarrow (\alpha_i, \boldsymbol{y}^*(\alpha_i)) \in \mathcal{C}^{new}_{piece}.$$

To predict the new active sets $\bar{\mathcal{I}}$, we proceed as follows. Let $\boldsymbol{y}^*(\alpha_{i-1}) = (\boldsymbol{u}^*, \boldsymbol{\lambda}^*_\nu, \boldsymbol{\lambda}^*_t) \in \mathbb{R}^{n+2m}$ be a solution to $(\boldsymbol{\mathcal{P}}(\bar{\alpha}_{i-1}))_{NE}$ and

$$M = \min_{i \in \mathcal{M}} \left\{ |\boldsymbol{\lambda}^*_\nu + \rho \mathbb{N} \boldsymbol{u}^*|_i, |\boldsymbol{\lambda}^*_t + \rho \mathbb{T} \boldsymbol{u}^* - \boldsymbol{\mathcal{F}} \odot \boldsymbol{\lambda}^*_\nu|_i, |\boldsymbol{\lambda}^*_t + \rho \mathbb{T} \boldsymbol{u}^* + \boldsymbol{\mathcal{F}} \odot \boldsymbol{\lambda}^*_\nu|_i \right\}.$$

One can expect that there is only one argument in $\{\,\}$ at which the minimum is attained for some $j \in \mathcal{M}$. This is realistic if $\delta_{\min}$ is small enough. The

index $j \in \mathcal{M}$ is moved ("$\overset{j}{\longleftrightarrow}$") from the active, inactive set to the inactive, and active set, respectively:

$$\left.\begin{array}{ll} \texttt{if} \;\; M = |\boldsymbol{\lambda}_\nu^* + \rho \mathbb{N} \boldsymbol{u}^*|_j, & \mathcal{A}_\nu \overset{j}{\longleftrightarrow} \mathcal{I}_\nu \\ \texttt{elseif} \;\; M = |\boldsymbol{\lambda}_t^* + \rho \mathbb{T} \boldsymbol{u}^* - \boldsymbol{\mathcal{F}} \odot \boldsymbol{\lambda}_\nu^*|_j, & \mathcal{A}_t \overset{j}{\longleftrightarrow} \mathcal{I}_t^+ \\ \texttt{elseif} \;\; M = |\boldsymbol{\lambda}_t^* + \rho \mathbb{T} \boldsymbol{u}^* + \boldsymbol{\mathcal{F}} \odot \boldsymbol{\lambda}_\nu^*|_j, & \mathcal{A}_t \overset{j}{\longleftrightarrow} \mathcal{I}_t^- \end{array}\right\} \quad \bar{\mathcal{I}} := \mathcal{I} \qquad (21)$$

This procedure results in an update of $\mathcal{I}$ denoted as $\bar{\mathcal{I}}$. Then we apply the predictor-corrector technique in order to find a point $(\alpha_i, \boldsymbol{y}^*(\alpha_i))$ belonging to $\mathcal{C}_{piece}^{new}$. The algorithm reads as follows:

Algorithm NSM (New Smooth Piece)

*(i)* Define: $\bar{\alpha} = \alpha_{i-1} + s\delta_{\min}$ and $\bar{\mathcal{I}}$ by (21);

*(ii)* Predictor-corrector: $\boldsymbol{y}^{(0)} = DirNeu(\bar{\mathcal{I}}, \bar{\alpha})$, $\boldsymbol{y}^{(\bar{k})} = SSNM(\boldsymbol{y}^{(0)}, \bar{\alpha})$;

*(iii)* Decision:

$$\begin{array}{rl} \texttt{if} & \bar{k} = 1,\ \alpha_i := \bar{\alpha},\ \boldsymbol{y}^*(\alpha_i) := \boldsymbol{y}^{(1)},\ \texttt{return} \\ \texttt{else} & \alpha_i := \alpha_{i-1},\ \boldsymbol{y}^*(\alpha_i) := DirNeu(\bar{\mathcal{I}}, \alpha_i),\ s := -s,\ \texttt{return}. \end{array}$$

If $\bar{k} = 1$, then the orientation $s$ remains the same and the algorithm identifies the transversal transition point; see Figure 3 *c)*. If $\bar{k} \neq 1$ then $s := -s$ and the algorithm identifies the turning transition point; see Figure 3 *d)*. The latter enables us to find multiple solutions. In this case it is sufficient to perform only the predictor step to get the solution $\boldsymbol{y}^*(\alpha_i)$ to $(\boldsymbol{\mathcal{P}}(\alpha_i))_{NE}$, since Assumption 1 excludes "vertical" pieces of any branch.

*5.3. Finding of further branches*

Our aim is to detect the solution path $\mathcal{C}$ parametrized by the coefficient of friction when

$$\mathcal{C} = \bigcup \mathcal{C}_p, \quad \mathcal{C}_p \cap \mathcal{C}_q = \emptyset, \quad p \neq q, \quad p \geq 2$$

i.e., $\mathcal{C}$ consists of several branches $\mathcal{C}_p$ that are not connected. The algorithm described in the previous parts enables us to perform the continuation along one branch. To find other branches we use the continuation by the load vector $\boldsymbol{L}$ as the auxiliary continuation process (see Figure 4 and compare with Figure 1).

We introduce two continuation parameters $\alpha$, $\beta$ and assume that the respective quantities are parametrized as follows:

$$\boldsymbol{L}(\alpha) := \alpha \boldsymbol{L}_1 + (1-\alpha)\boldsymbol{L}_2, \quad \alpha \in [\alpha_{\min}, \alpha_{\max}], \tag{22}$$

$$\boldsymbol{\mathcal{F}}(\beta) := \beta \boldsymbol{\mathcal{F}}_0, \quad \beta \in [\beta_{\min}, \beta_{\max}], \tag{23}$$

where $\boldsymbol{L}_1$, $\boldsymbol{L}_2$, and $\boldsymbol{\mathcal{F}}_0$ are appropriate vectors. Since we combine the continuation with respect to $\alpha$ and $\beta$ we shall denote by $\boldsymbol{y}^*(\alpha, \beta)$ any solution to $(\boldsymbol{\mathcal{P}})_{NE}$ with the load vector $\boldsymbol{L} \equiv \boldsymbol{L}(\alpha)$ and the coefficient of friction $\boldsymbol{\mathcal{F}} \equiv \boldsymbol{\mathcal{F}}(\beta)$. Our aim is to continue the solution to $(\boldsymbol{\mathcal{P}})_{NE}$ by $\beta \in [\beta_{\min}, \beta_{\max}]$ for a fixed load $\boldsymbol{L}(\bar{\alpha})$, $\bar{\alpha} \in [\alpha_{\min}, \alpha_{\max}]$. Let $\beta_{\min}$ be sufficiently small so that $(\boldsymbol{\mathcal{P}})_{NE}$ has a unique solution $\boldsymbol{y}^*(\alpha, \beta_{\min})$ for any $\alpha \in [\alpha_{\min}, \alpha_{\max}]$ (even for any $\alpha \in \mathbb{R}$ as follows from Remark 2). The continuation procedure consists of the following steps:

*(i)* Compute the initial point $Q_0 = (\beta_{\min}, \boldsymbol{y}^*(\bar{\alpha}, \beta_{\min})) \in \mathcal{C}_1$;

*(ii)* Perform the continuation along $\mathcal{C}_1$ by $\beta \in [\beta_{\min}, \beta_{\max}]$ starting from $Q_0$ with the orientation $s = 1$;

*(iii)* Chose sufficiently large $\bar{\beta} \in [\beta_{\min}, \beta_{\max}]$ for which one can expect multiple solutions and compute $Q_1 = (\bar{\beta}, \boldsymbol{y}_1^*(\bar{\alpha}, \bar{\beta})) \in \mathcal{C}_1$. Perform the continuation along the solution path $\mathcal{C}_{load}$ (tiny line) starting from $Q_1' = (\bar{\alpha}, \boldsymbol{y}_1^*(\bar{\alpha}, \bar{\beta})) \in \mathcal{C}_{load}$ with $s = 1$ as well as $s = -1$, i.e. for $\alpha \in [\bar{\alpha}, \alpha_{\max}]$ and $\alpha \in [\alpha_{\min}, \bar{\alpha}]$. Find as much points $Q_p' = (\bar{\alpha}, \boldsymbol{y}_p^*(\bar{\alpha}, \bar{\beta})) \in \mathcal{C}_{load}$, $p = 2, 3, \dots$ as possible (denoted by $\odot$ in Figure 4). Since pieces of $\mathcal{C}_{load}$ are affine, one can interpolate multiple solutions exactly at $\bar{\alpha}$ from the sequence of continuation points along $\mathcal{C}_{load}$;

*(iv)* Perform the continuation along the branch $\mathcal{C}_p$ ($p = 2, 3, \dots$) by $\beta \in [\beta_{\min}, \beta_{\max}]$ starting from $Q_p = (\bar{\beta}, \boldsymbol{y}_p^*(\bar{\alpha}, \bar{\beta})) \in \mathcal{C}_p$ with $s = 1$ as well as $s = -1$, i.e. for $\beta \in [\bar{\beta}, \beta_{\max}]$ and $\beta \in [\beta_{\min}, \bar{\beta}]$;

*(v)* Identify $\mathcal{C}_p$ and $\mathcal{C}_q$, $p \neq q$ representing the same branch of $\mathcal{C}$. Consider one of them.

Note that steps *(iii)* and *(v)* require an interactive treatment. The other steps are automatically implemented by the continuation algorithm described in the previous subsections and by the semismooth Newton method.

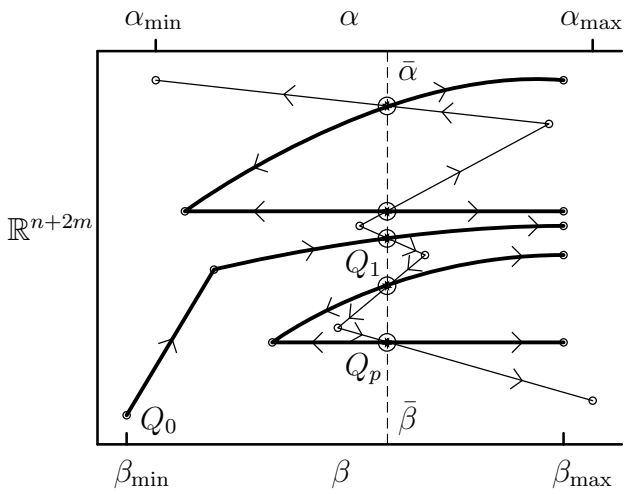


Figure 4: Combination of continuations by $\boldsymbol{\mathcal{F}}$ and $\boldsymbol{L}$.

## 6. Computational experiments

*6.1. Model problem*

Let us consider the problem (1)-(7) with the following data. Two plane elastic bodies $\Omega^1 = (0,3) \times (1,2)$, $\Omega^2 = (0,3) \times (0,1)$ are characterized by the Young modulus $E^1 = 2.1 \cdot 10^9$, $E^2 = 2.1 \cdot 10^{11}$ and the Poisson ratio $\sigma^1 = \sigma^2 = 0.28$. The boundaries of $\partial\Omega^1$ and $\partial\Omega^2$ are decomposed follows: $\Gamma_u^1 = \{0\} \times (1,2)$, $\Gamma_c^1 = (0,3) \times \{1\}$, $\Gamma_f^1 = \partial\Omega^1 \setminus \overline{\Gamma_u^1 \cup \Gamma_c^1}$ and $\Gamma_u^2 = \{0\} \times (0,1)$, $\Gamma_c^2 = \Gamma_c^1$, $\Gamma_f^2 = \partial\Omega_2 \setminus \overline{\Gamma_u^2 \cup \Gamma_c^2}$, respectively (see Figure 5). The surface tractions of density $\boldsymbol{f}_{1|\Gamma_f^1} = (f_{1x}, f_{1y})$, $\boldsymbol{f}_{2|\Gamma_f^1} = (f_{2x}, f_{2y})$ which act on $\Gamma_f^1$ define the load vectors $\boldsymbol{L}_1$ and $\boldsymbol{L}_2$ in (22), respectively, are given by:

$$
\begin{aligned}
&f_{1x}(x,2) = 0, \quad x \in (0,3),\\
&f_{1y}(x,2) = f_{1y,L} + f_{1y,R}\, x, \quad x \in (0,3),\\
&f_{1x}(3,y) = f_{1x,B}(2-y) + f_{1x,U}\,(y-1), \quad y \in (1,2),\\
&f_{1y}(3,y) = f_{1y,B}(2-y) + f_{1y,U}\,(y-1), \quad y \in (1,2)
\end{aligned}
$$

with $f_{1y,L} = -6 \cdot 10^7$, $f_{1y,R} = -1 \cdot 10^7$, $f_{1x,B} = f_{1x,U} = f_{1y,U} = 2 \cdot 10^7$, $f_{1y,B} = 4 \cdot 10^7$ and

$$
\begin{aligned}
&f_{1x}(x,2) = 0, \quad x \in (0,3),\\
&f_{2y}(x,2) = f_{2y,L} + f_{2y,R}\, x, \quad x \in (0,3),\\
&f_{2x}(3,y) = f_{2x,B}(2-y) + f_{2x,U}\,(y-1), \quad y \in (1,2),\\
&f_{2y}(3,y) = f_{2y,B}(2-y) + f_{2y,U}\,(y-1), \quad y \in (1,2),
\end{aligned}
$$

where $f_{2y,L} = -5 \cdot 10^7$, $f_{2y,R} = -2 \cdot 10^7$, $f_{2x,B} = f_{2x,U} = f_{2y,U} = 2 \cdot 10^7$, and $f_{2y,B} = 4 \cdot 10^7$, respectively. All entries of the vector $\boldsymbol{\mathcal{F}}_0$ in (23) are equal to one. Further $\alpha \in \langle 1.2, 2\rangle$ and $\beta \in \langle 0.3, 35\rangle$. Finally, in most of cases is $\bar{\beta} = 15$, exceptions will be quoted explicitly. The problem is discretized by the triangulations of $\overline{\Omega}^1$ and $\overline{\Omega}^2$ as seen in Figure 5 for which $n = 1320$ (the total number of the nodal displacements) and $m = 30$ (the number of the contact nodes). Algorithm PC and NSM use the following stepsize parameters: $\delta_{\min} = 10^{-5}$, $\delta_{\max} = 5$, $c_p = 1.3$, and $c_s = 0.5$.

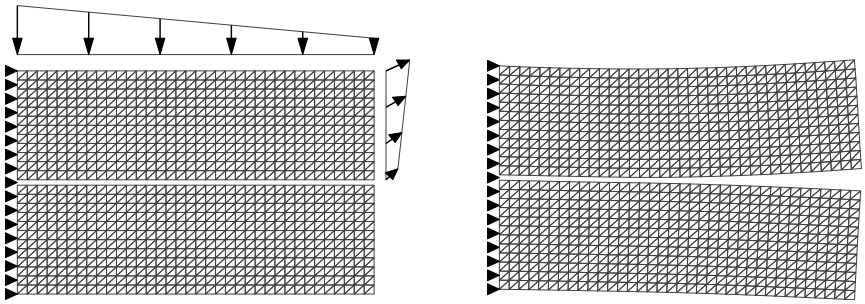


Figure 5: *a)* two elastic bodies $\Omega^1$ (the upper body) and $\Omega^2$ in contact along $\Gamma_c$; *b)* deformed configuration.

*6.2. Results of the continuation algorithm*

The aim of this part is to find a structure of solutions to $(\boldsymbol{\mathcal{P}}(\beta))_{NE}$ parametrized by $\boldsymbol{\mathcal{F}}(\beta)$ with the fixed load $\boldsymbol{L}(\bar{\alpha})$, $\bar{\alpha} = 1.6$. Since we want to find possible disconnected solution branches, we also use a continuation with respect to $\alpha$ as described in Subsection 5.3. The resulting branches will be visualized as plots of the continuation parameters $\alpha$, $\beta$ versus the normal,

tangential stresses $\boldsymbol{\lambda}_\nu(i)$, $\boldsymbol{\lambda}_t(i)$ and the normal displacement $(\mathbb{N}\boldsymbol{u})(i)$ at the $i$-th contact node, respectively.

Figure 6 shows the behavior of $\boldsymbol{\lambda}_t(1)$ as a function of $\alpha$ for the fixed coefficient of friction $\boldsymbol{\mathcal{F}}(\bar{\beta})$, $\bar{\beta} = 6$ *(a)* and $\bar{\beta} = 15$ *(b)*. A zoom of the branch for $\bar{\beta} = 15$ is presented in Figure 7. The vertical line at $\bar{\alpha} = 1.6$ has five intersections with the piecewise affine curve. These points determine five different solutions $\boldsymbol{y}_p^*(\bar{\alpha})$, $p = 1, \ldots, 5$ for $\bar{\alpha} = 1.6$. Any solution $\boldsymbol{y}_p^*(\bar{\alpha})$ has to be understood as a point in $\mathbb{R}^{n+2m}$, in our case $n = 1320$ and $m = 30$, and it will be identified through the respective $\boldsymbol{\lambda}_t(1)$.

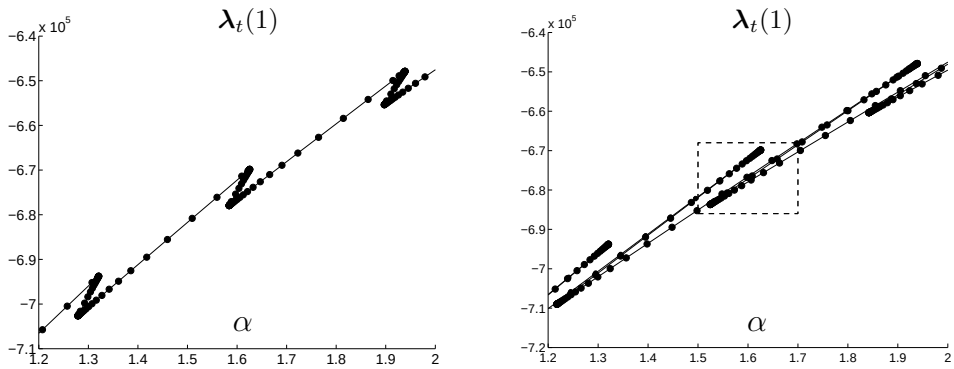


Figure 6: $\boldsymbol{\lambda}_t(1)$ as a function of $\alpha$ for $\bar{\beta} = 6$ *(a)* and $\bar{\beta} = 15$ *(b)*.

Since we want to find different branches of the problem parametrized by the coefficient of friction, i.e. by $\beta$ (if they exist), the solutions $\boldsymbol{y}_p^*(\bar{\alpha})$, $p = 1, \ldots, 5$ are used as the starting points in the continuation algorithm for $\beta$. We found three branches representing the evolution of the normal stress $\boldsymbol{\lambda}_\nu(19)$, see Figure 8. Branch 1 is initiated at $\boldsymbol{y}_1^*(\bar{\alpha})$. Branch 2 starts from $\boldsymbol{y}_2^*(\bar{\alpha})$ and contains also $\boldsymbol{y}_5^*(\bar{\alpha})$. Finally Branch 3 is initiated at $\boldsymbol{y}_3^*(\bar{\alpha})$ and contains also $\boldsymbol{y}_4^*(\bar{\alpha})$. The respective normal contact stress $\boldsymbol{\lambda}_\nu(19)$ corresponding to $\boldsymbol{y}_p^*(\bar{\alpha})$, $p = 1, \ldots, 5$ is denoted by $\odot$. The branches are continued in both, the negative ($s = -1$) and positive ($s = 1$) directions. These figures also illustrate the step-size control. We see that the continuation algorithm needs tiny steps in the vicinity of the starting and the transition points. The collection of all three branches represents the solution path, or at least its part.

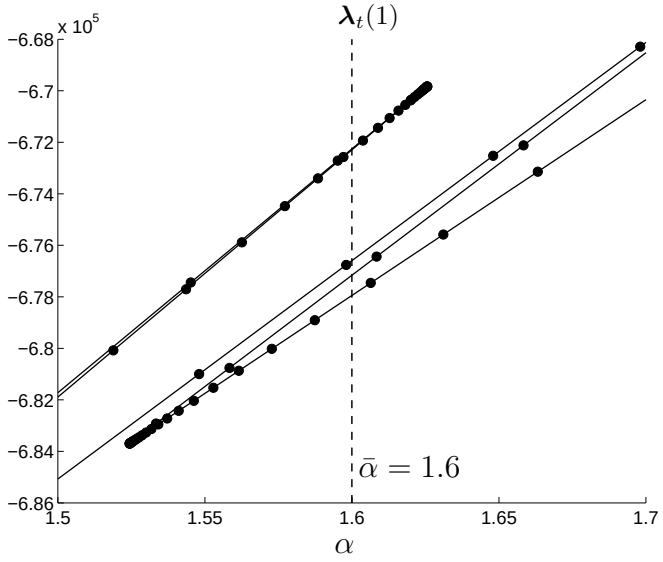


Figure 7: A zoom of Figure 6 *(b)*; five different solutions $\boldsymbol{y}_p^*(\bar{\alpha})$ determined by $\boldsymbol{\lambda}_t(1)$, $p = 1, \ldots, 5$ for $\bar{\alpha} = 1.6$ and $\bar{\beta} = 15$ (with close values $\boldsymbol{\lambda}_t(1)$ at the upper pieces).

Figure 9 depicts the solution path represented by the evolution (with respect to $\beta$) of the normal stress at the contact nodes No.19, 20, 21, and the normal displacement at the node 22. A contact node *(i)* is termed *no-contact*, *contact-stick*, *contact-slip* point, if $(\mathbb{N}\boldsymbol{u})(i) < 0$, $\boldsymbol{\lambda}_\nu(i) < 0$ & $|\boldsymbol{\lambda}_t(i)| < -\mathcal{F}\boldsymbol{\lambda}_\nu(i)$, and $\boldsymbol{\lambda}_\nu(i) < 0$ & $(\mathbb{T}\boldsymbol{u})(i) \neq 0$, respectively. To distinguish the individual pieces consisting of no-contact, contact-stick and contact-slip points we use solid, dashed and dash-dotted lines, respectively. Note the presence of the transversal and turning transition points in Figure 9. The existence of such points entails qualitative changes of the solution. Finally, the path at the contact node 22 consists only of no-contact points. The corresponding branches at the different contact nodes are labeled by the same number, i.e., if $k$ denotes a branch at the (reference) contact node No.19, then the corresponding branches at the remaining nodes are denoted by $k$, as well.

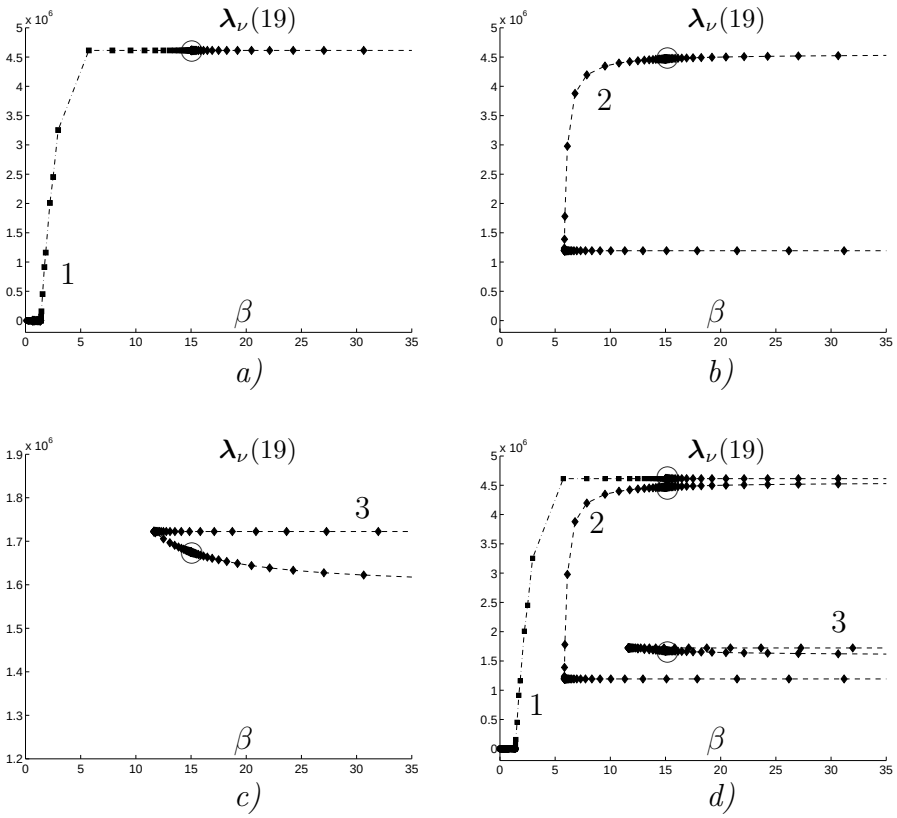


Figure 8: Three branches of $\boldsymbol{\lambda}_\nu(19)$: Branch 1 *(a)*, Branch 2 *(b)*, Branch 3 *(c)*, the solution path *(d)* (all three branches).

## 7. Conclusions

We proposed a new continuation technique for numerical analysis of parameter-dependent contact problems with Coulomb friction. In particular, the method was applied to continue solution branches parametrized by the coefficient of friction.

The branches are naturally parametrized by a chosen continuation parameter. The branch consists of smooth pieces which are connected by transition points. To each piece an orientation (either 1, or $-1$) is assigned. We distinguish transversal and turning transition points. At the former, the branch does not change its orientation while at the latter does. At turning transition points solutions undergo a qualitative change.

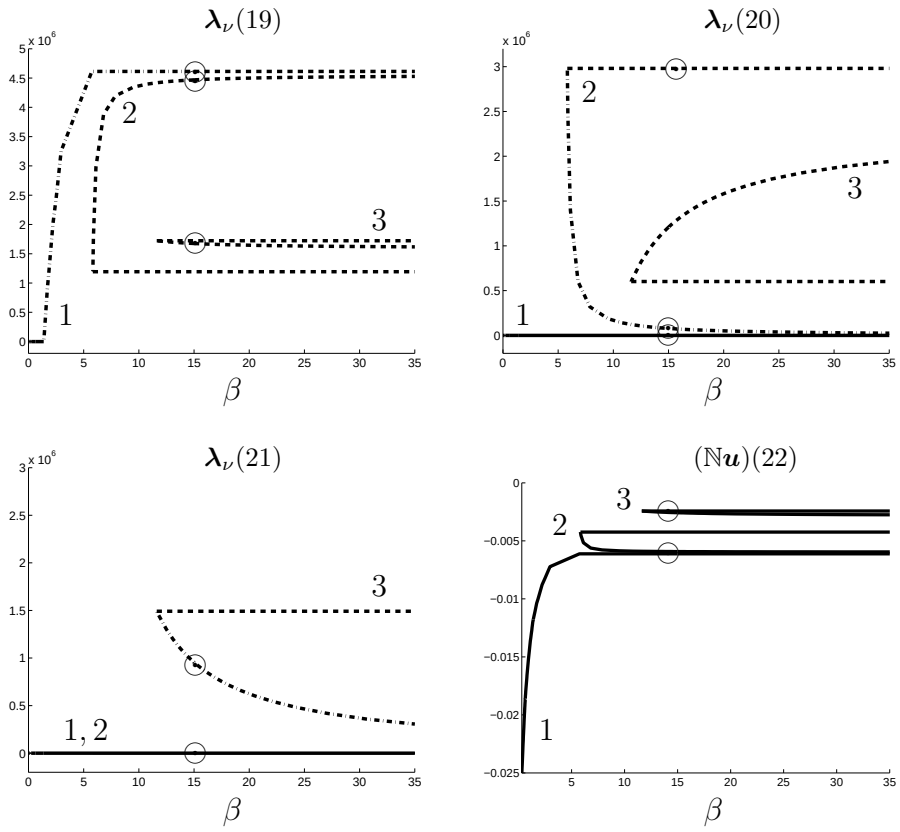


Figure 9: The evolution of the normal stress at the contact node No. 19-21 and the normal displacement at the contact node No.22 (solid line: no contact, dashed line: contact stick, dash-dotted line: contact-slip).

From the algorithmic point of view, the smooth pieces are continued according to Algorithm PC (Predictor-Corrector), with an adaptive stepsize control. The transition points are processed by Algorithm NSM (New Smooth Piece). The active/inactive set strategy of the semismooth Newton method is used. Numerical experiments confirmed the reliability of the proposed continuation algorithm.

*Acknowledgement*

This work was supported by the grant GAČR P201/12/0671. The third author also acknowledges the European Development Fund in the IT4Innovations

Centre of Excellence project CZ.1.05/1.1.00/02.0070.

## References

[1] P. Alart, A. Curnier, A mixed formulation for frictional contact problems prone to Newton like solution methods, Comput. Methods Appl. Mech. Engrg. 92 (1991) 353–375.

[2] E.L. Allgower, K. Georg, Numerical Path Following, Handbook of numerical analysis vol. V, Elsevier Science, New York, 1997.

[3] X. Chen, Z. Na shed, L. Qi, Smoothing methods and semismooth methods for non-differentiable operator equations, SIAM J. Numer. Anal. 38 (2000) 1200–1216.

[4] P. Deuflhart, A. Hohmann, Numerical Analysis in Modern Scientific Computing, Texts in Applied Mathematics, Springer Verlag, New York, 2003.

[5] A. Dhooge, W. Govaerts, Y. A. Kuzetsov, MATCONT: A Matlab package for numerical bifurcation analysis of ODEs, ACM Transactions on Mathematical Software 31 (2003) 141-164.

[6] C. Eck, J. Jarušek, M. Krbec, Unilateral Contact Problems: Variational Methods and Existence Theorems, Chapman&Hall/CRC Press, Boca Raton, 2005.

[7] R. Glowinski, Numerical Methods for Nonlinear Variational Problems, Springer Series in Computational Physics, Springer Verlag, 1984.

[8] J. Haslinger, Approximation of the Signorini problem with friction obeying the Coulomb law, Math. Methods in Appl. Sci. 5 (1983) 422-437.

[9] J. Haslinger, V. Janovský, R. Kučera, Path-following the static contact problem with Coulomb friction, in J. Brandts, S. Korotov, M. Křížek, J. Šístek, T. Vejchodský (Eds) Proceedings of the International Conference Applications of Mathematics 2013, Institute of Mathematics, Academy of Sciences of the Czech Republic, Prague 2013, pp. 104–116.

[10] J. Haslinger, V. Janovský, T. Ligurský, Qualitative analysis of solutions to discrete static contact problems with Coulomb friction, Comp. Meth. Appl. Mech. Engrg. 205-208 (2012) 149-161.

[11] J. Haslinger, I. Hlaváček, and J. Nečas, Numerical Methods for Unilateral Problems in Solid Mechanics, in P.G. Ciarlet, J.L. Lions (Eds), Handbook of Numerical Analysis, Vol. IV, Part 2, North-Holland, Amsterdam, 1996, pp. 313–485.

[12] J. Haslinger, R. Kučera, T. Ligurský, Qualitative analysis of 3D elastostatic contact problems with orthotropic Coulomb friction and solution-dependent coefficients of friction, J. Comput. Appl. Math. 235 (2011) 3464–3480.

[13] P. Hild, Non-unique slipping in the Coulomb friction model in two dimensional linear elasticity, Q. J. Mech. Appl. Math. 57 (2004) 225–235.

[14] P. Hild, Y. Renard, Local uniqueness and continuation of solutions for the discrete Coulomb friction problem in elastostatics, Quart. Appl. Math. 63 (2005) 553–573.

[15] M. Hintermüller, K. Ito, K. Kunisch, The primal-dual active set strategy as a semismooth Newton method, SIAM J. Optim. 13 (2003) 865-888.

[16] V. Janovský, T. Ligurský, Computing non unique solutions of the Coulomb friction problem, Math. Comput. Simul. 82 (2012) 20472061.

[17] J. Katzenelson, An algorithm for solving nonlinear resistor networks, Bell. Syst. Tech. J. 44 (1965) 1605–1620.

[18] T. Ligurský, Theoretical analysis of discrete contact problems with Coulomb friction, Appl. Math. 57 (2012) 263–295.

[19] T. Ligurský, Y. Renard, A continuation problem for computing solutions of discretised evolution problems with application to plane quasistatic contact problems with friction, Comp. Meth. Appl. Mech. Engrg. 280 (2014) 222-262.

[20] J. Outrata, M. Kočvara, J. Zowe, Nonsmooth Approach to Optimization Problems with Equilibrium Constraints: Theory, Applications and Numerical Results, Kluwer Academic Publisher, London, 1998.

[21] Y. Renard, A uniqueness criterion for the Signorini problem with Coulomb friction, Lect. Notes Appl. Comput. Mech. 27 (2006) 161–169.

[22] S. Scholtes, Introduction to Piecewise Differentiable Equations, Springer, Berlin, 2012.